

https://dspace.org/

Flow resistance in open channels with intermediate scale roughness

Mashau, Mashau Samson

2007-02-22T11:02:38Z
http://hdl.handle.net/10539/2077

Downloaded from a DSpace repository. https://dspace.org/

FLOW RESISTANCE IN OPEN CHANNELS WITH INTERMEDIATE SCALE ROUGHNESS

Mashau Samson Mashau

A research report submitted to the Faculty of Engineering and the Built Environment, University of Witwatersrand, in fulfillment of the degree of Master of Science in Engineering.

Johannesburg 2006

ABSTRACT

Many environmental and engineering projects require prediction of the velocity of flow in river channels, in terms of those channel properties and flow characteristics which induce resisting forces or an energy loss to the flow. Relationships such as the Manning, Chézy and Darcy-Weisbach equations have been in use for a century or more. All of them account for resistance with a single coefficient of resistance, and the central problem is evaluation of this coefficient.

Experimental results by different researchers have shown that Manning's n varies strongly with the ratio of flow depth to roughness height. It is constant for values of this ratio above about 4, but increases significantly for lower values. This suggests that the equation is not suitable in its original form for the case of intermediate-scale roughness. The roughness is intermediate-scale if the relative submergence ratio of flow depth to roughness elements height lies between 1 and 4. The influence of the roughness elements on flow resistance in this regime is caused by a combination of both element drag and boundary shear, or friction.

The results of an experimental study with hemispherical roughness elements are presented, showing how the roughness element size, spacing and pattern influence flow resistance. For the range of conditions tested, Manning's n appears to depend on roughness element size, spacing and pattern.

ACKNOWLEDGEMENTS

The supervisor of this research was Professor C.S James and the co-supervisor was Mrs. A.A Jordanova. I wish to thank them for advice and support during the work.

Furthermore, I would like to thank National Research Foundation (NRF) for awarding a scholarship and Council for Scientific and Industrial Research (CSIR) for awarding a bursary.

Special thanks go to my lovely family and fabulous friends, especially Peter Hirschowitz and Maurice Nwendabai who have helped, supported, and believed in me during this work. Very special thanks go to God knows Njowa for his great support and encouragement.

LIST OF TABLES

Table 1.1 Three roughness scales

Table 2.1 Recommended values of effective roughness, k_s

Table 4.1 Hydraulic parameters and friction factor of the bed for Series A

Table 4.2 Hydraulic parameters and friction factor of the bed for Test 2

Table 4.3 Hydraulic parameters and friction factor of the bed for Test 3

Table 4.4 Hydraulic parameters and friction factor of the bed for Test 4

Table 4.5 Hydraulic parameters and friction factor of the bed for Test 5

Table 4.6 Hydraulic parameters and friction factor of the bed for Test 6

Table 4.7 Hydraulic parameters and friction factor of the bed for Test 7

Table 4.8 Hydraulic parameters and friction factor of the bed for Test 8

Table 4.9 Hydraulic parameters and friction factor of the bed for Test 9

Table 4.10 Experimental conditions for series A, B, C and D experiments

Table 5.1 The Manning's and Strickler's n values

Table 5.2 Values of coefficients a and b for the different condition

Table 5.3 Fitted and ignored data when plotting Figure 5.10

Table 5.4 Fitted and ignored data when plotting Figure 5.14

Table 5.5 Experimental data used for verification of proposed equation (5.13)

Table 5.6 Velocity prediction errors in application of proposed equation (5.13) for series B, C and D

Table 5.7 Velocity prediction errors in application of proposed equation (5.13) for conditions listed in Table 5.5

LIST OF FIGURES

Figure 3.1 Tilting-glass walled flume

Figure 3.2 Example of hemispherical roughness elements

Figure 3.3 Example of staggered pattern

Figure 3.4 Example of parallel pattern

Figure 4.1 Effect of roughness element size on flow resistance

Figure 4.2 A plot of friction factor of a bed against the flow depth for Tests 3 and 6

Figure 4.3 Effect of roughness element spacing on flow resistance

Figure 4.4 A plot of friction factor of a bed against the flow depth for Tests 5 and 8

Figure 4.5 Effect of roughness element pattern on flow resistance

Figure 4.6 A plot of friction factor of a bed against the flow depth for Tests 3 and 4

Figure 5.1 Comparison of Manning's n for Stickler's equation against effective surface roughness height

Figure 5.2 A plot of Manning's n against the relative submergence for Test 2

Figure 5.3 A plot of Manning's n against the relative submergence for Test 3

Figure 5.4 A plot of Manning's n against the relative submergence for Test 4

Figure 5.5 A plot of Manning's n against the relative submergence for Test 5

Figure 5.6 A plot of Manning's n against the relative submergence for Test 6

Figure 5.7 A plot of Manning's n against the relative submergence for Test 7

Figure 5.8 A plot of Manning's n against the relative submergence for Test 8

Figure 5.9 A plot of Manning's n against the relative submergence for Test 9

Figure 5.10 A plot of coefficient a against the ratio of diameter to spacing of hemispheres

Figure 5.11 A plot of coefficient b against the area coverage of hemispheres

Figure 5.12 A plot of coefficient b against ratio of diameter to spacing of hemispheres

Figure 5.13 A plot of coefficient a against area coverage of hemispheres

Figure 5.14 A plot of coefficient b against diameter of hemispheres

Figure 5.15 Comparison of the measured and predicted velocities for series B, C and D

Figure 5.16 Comparison of the measured and predicted Manning resistance coefficients for Series B, C and D

Figure 5.17 Comparison of the measured and predicted velocities for the conditions listed in Table 5.3

LIST OF SYMBOLS AND ABBREVIATIONS

a	coefficient related to the relative submergence
A	cross-sectional area
ABS	absolute
AC	area covered by roughness element
a	spacing
b	coefficient related to the relative submergence
D	particle diameter
D	roughness element diameter
D_s	particle size
f	Darcy-Weisbach friction factor
f_b	friction factor (bed)
f_w	friction factor (wall)
g	gravitational acceleration
h	roughness element height
k_s	Nikuradse roughness
n	Manning's roughness coefficient
n_b	Manning's roughness coefficient (bed)
n_m	Manning's roughness coefficient (measured)
n_p	Manning's roughness coefficient (predicted)
n_s	Strickler's n values
n_w	Manning's roughness coefficient (wall)
P	wetted perimeter
R	hydraulic radius
R_b	hydraulic radius (bed)

R_e	Reynolds number
Re_*	shear Reynolds number
R_{eb}	Reynolds number (bed)
S	slope of the channel
Sp	roughness element spacing
U_*	shear velocity
V	average velocity
V_m	average velocity (measured)
V_p	average velocity (predicted)
y	flow depth

CONTENTS

ABSTRACT		i
ACKNOWLEDGEMENTS		ii
LIST OF TABLES		iii
LIST OF FIGURES		iv
LIST OF SYMBOLS AND ABBREVIATIONS		vi
TABLE OF CONTENTS		viii
1	**INNTRODUCTION**	1
1.1	Background	1
1.2	Aim and Objectives	3
1.3	Statement of the Problem	3
1.4	Research Hypothesis	4
1.5	Research Question	4
2	**LITERATURE REVIEW**	5
2.1	Flow Resistance in Open Channels	5
2.2	Flow Resistance Equations	6
2.3	Roughness Characteristics	12
2.3.1	Roughness Size	12
2.3.2	Roughness Shape	12
2.3.3	Roughness Size Distribution	13
2.3.4	Roughness Spacing	14
3	**LABORATORY EXPERIMENTS**	15
3.1	Experimental Facilities	15
3.2	Experimental Parameters	16

3.3	Experimental Procedure	18
3.4	Test Series Description	18
3.4.1	Series A Experiments	19
3.4.2	Series B Experiments	19
3.4.3	Series D Experiments	19
3.4.4	Series E experiments	19
3.5	Side-Wall Correction Procedure	21
3.6	The Effective Roughness of the Bed	23
4	**RESULTS AND DISCUSSION**	24
4.1	Experimental Results	24
4.1.1	Series A Experimental Results	24
4.1.2	Series B Experimental Results	25
4.1.3	Series C Experimental Results	27
4.1.4	Series D Experimental Results	29
4.2	Influence of Roughness Element Size on Flow Resistance	30
4.3	Influence of Roughness Element Spacing on Flow Resistance	32
4.4	Influence of Roughness Element Pattern on Flow Resistance	34
4.5	Conclusion	36
5	**ANALYSIS AND PREDICTIVE RESULTS**	37
5.1	Flow Resistance Prediction	37
5.1.1	Flow Resistance of Small Scale Roughness	37
5.1.2	Flow Resistance of Intermediate-Scale Roughness	39
5.2	Verification of Proposed Equation	44
6	**CONCLUSIONS**	55
7	**REFERENCES**	56

APPENDIX 59

DECLARATION

I declare that this research report is my own work. It is being submitted for the degree of Master of Science in Engineering in the University of Witwatersrand, Johannesburg. It has not been submitted before for any degree or examination in any other University.

_____

(Signature of candidate)

_____ day of _____ 2006

CHAPTER 1: INTRODUCTION

1. Introduction

1.1. Background

The management of rivers requires understanding of the processes and phenomena underlying their behaviour, including the relationship between discharge and characteristics of local hydraulics.

The prediction of the velocity of flow in river channels is of concern to many environmental scientists and engineers. Local flow depths and velocities are determined by flow resistance, which is conventionally described by well-known equations, in terms of those channel properties and flow characteristics which induce resisting forces or an energy loss to the flow. However, these equations are not adequate for some conditions particularly intermediate-scale roughness (Jordanova et. al, 2004).

An attempt has been made to characterize the scale of the flow resistance in terms of the relative submergence (ratio of flow depth to height of roughness elements), $\frac{y}{D_s}$

(y = mean flow depth, D_s = characteristic size of bed material). The relative submergence of a river is classified into small-scale, intermediate-scale and large-scale depending on the bed material sizes and the flow condition (Bathurst, 1978; Thorne and Zevenbergen, 1985; French, 1985).

The roughness is small-scale if the relative submergence ratio of flow depth to roughness elements height exceeds about 4 (Jordanova et. al, 2004). In flow resistance of small-scale roughness, the boundary resistance is the result of shear and

pressure forces acting on the grains comprising the boundary, and the applied force per unit plan area is balanced by resisting forces.

The roughness is intermediate-scale if the relative submergence ratio of flow depth to roughness elements height, lies between 1 and about 4 (Jordanova et. al, 2004). This regime represents a state of flow in which the influence of the roughness elements on flow resistance is manifest as a combination of both element drag and boundary shear, or friction.

The roughness is large-scale if the relative submergence ratio of flow depth to roughness elements height is less than 1 (Jordanova et. al, 2004). The height of large-scale roughness elements is associated with very complex interaction between roughness element drag, wake vortices and local hydraulic jumps (Jordanova et. al., 2004).

Natural river beds are composed of roughness elements of different sizes, and bed roughness should be represented by a single characteristic size, such as D_{50} or D_{84}. Three roughness scales based on relative submergence and bed material sizes are shown in Table 1.1 (Bathurst et al., 1982).

Table 1.1: Three Roughness Scales

Small-Scale Roughness	Intermediate-Scale Roughness	Large-Scale Roughness
$\frac{y}{D_{50}} > 7.5$	$2 < \frac{y}{D_{50}} < 7.5$	$\frac{y}{D_{50}} < 2$
$\frac{y}{D_{84}} > 4$	$1.2 < \frac{y}{D_{84}} < 4$	$\frac{y}{D_{84}} < 1.2$

where D_{50} is the median particle size, and D_{84} is the 84-percentile size of the median axis length.

Bayazit (1976) found from laboratory experiments that once the relative submergence exceeds a value of 3.3 in terms of D_{84}, the resistance of the flow is higher than that predicted by the logarithmic resistance equation (2.6) for small-scale roughness. Therefore the resistance equations for small-scale roughness are not appropriate for intermediate-scale condition because the associated resistance processes are different from those for small-scale roughness. When the relative submergence lies between 1 and 3.3, both drag and friction contribute significantly to flow resistance and the roughness is intermediate-scale.

The theory developed by Bathurst (1982) suggests that the resistance coefficient should vary with relative roughness, roughness shape, size distribution and spacing as well as channel geometry (bends, irregularities, obstructions). The channel geometry is also related to internal distortion resistance (wave resistance) and spill resistance. Wave resistance depends on distortions of the free surface and the effect of the free surface on turbulence structure and affects the near surface profile (Bathurst, 1982).

Channels with very tight inner bends exhibit an additional energy loss mechanism called spill resistance (Leopold et al., 1960). This results from sudden expansion of local supercritical flow induced by curvature of large-scale roughness elements, including the convex banks of sharp bends. Spill resistance is probably uncommon in natural and most designed bend geometries, but its effect is significant and should be taken cognizance of under low conditions in boulder bed rivers (James and Myers, 2002).

1.2. Aim and Objectives

The major aim of this project is to improve the prediction of flow resistance in open channels under condition of intermediate-scale roughness.

1.3. Statement of the problem

Relationships such as the Manning, Chézy and Darcy-Weisbach equations have been in use for a century or more. All of them account for resistance process with a single coefficient of resistance and the central problem is evaluation of this coefficient. The few investigations of flow resistance in open channels that have been conducted indicate that the equations for small-scale roughness are not suitable for intermediate-scale roughness, because the resistive processes are different in the two cases (Bathurst, 1978).

1.4. Research Hypothesis

It is hypothesized that the size, spacing and pattern of roughness elements influence flow resistance under intermediate roughness condition.

1.5. Research Question

The question that this project intended to answer is: How do the size, spacing and pattern of roughness elements influence flow resistance? This question has been answered by carrying out a laboratory flume study.

CHAPTER 2: LITERATURE REVIEW

2. Literature Review

2.1. Flow Resistance in Open Channels

An open channel is a conduit in which water flows with a free surface. The classification of open channel flow is made according to the change in flow depth with respect to time and space (Chadwick and Morfett, 1993).

The theoretical aspects of open channel flow resistance are documented in some publications such as Leopold et al (1960), Rouse (1965), Bathurst (1982) and Yen (2002). There are several components that contribute to flow resistance in an open channel, all of which contribute to the total flow resistance or roughness.

The four contributing components of flow resistance are classified by Yen (2002) as follows:

- Skin friction
- Form resistance
- Wave resistance
- Flow unsteadiness

Skin friction resistance depends on the roughness of the surface materials, and influences the near surface flow. Form resistance is caused by the separation of flow and secondary circulation. Both skin friction and form resistance combine to form boundary resistance. Boundary resistance depends on the bed material properties and influences the flow condition.

Wave resistance depends on distortions of the free surface instabilities such as roll waves that can affect the shape of the near surface velocity profile (Bathurst, 1982). The distortion of the free surface is also caused by large roughness elements and bed forms. Bathurst (1982) assumed that wind effects are negligible and found that the effect of large roughness elements and bed forms is insignificant in gravel-bed rivers under small-scale roughness condition. Flow unsteadiness is associated with longitudinal flow accelerations and decelerations.

The flow resistance of a channel is also significantly increased by the presence of bends (bend resistance). The additional resistance is the result of the development of secondary circulation as flow progress through a bend. The bends result in increased internal distortion resistance and sometimes spill resistance. Spill resistance is probably uncommon in natural and most designed bend geometries, but its effect is significant and should also be taken cognizance of under low flow conditions in boulder bed rivers (James and Myers, 2002).

2.2. Flow Resistance Equations

Flow resistance is a term used to describe the net effect of forces driving and resisting the movement of water. Yen (2002) defines hydraulic resistance as "the force to overcome or the work required to be done to counter the action of the rigid, flexible, or moving boundary on the flow."

Flow resistance describes influences of friction on the flow due to channel characteristics which influence the ability of a channel to carry flow. Examples of such characteristics include:

- Slope of the channel
- Bed friction which can be caused by bed material (e.g. sand, gravel, rock etc), vegetation, debris etc.

- Bank friction which can also be caused by vegetation, debris etc.
- Size and shape of the channel

The problem of flow resistance concerns the prediction of the velocity of flow, in terms of those channel properties and flow characteristics which act as a resistance or an energy loss to the flow (Bathurst, 2002). The three popular relationships linking velocity and flow resistance are the Chézy, Manning and Darcy-Weisbach formulae.

The first significant attempt to obtain flow resistance relationship was made by Chézy in about 1768, who proposed equation (2.1).

$$V = C\sqrt{RS} \qquad 2.1$$

where V = velocity of flow, C = Chézy resistance coefficient, R = hydraulic radius (= A/P where A is the cross-sectional area and P is the wetted perimeter), S = slope.

Over many years the application of the Chézy equation made it apparent that C was not constant, even for the same channel, but varied with flow condition (James and Myers, 2002). The problem was addressed by many researchers and C was eventually related to the shape and size of the channel by equation (2.2).

$$C = \frac{R^{1/6}}{n} \qquad 2.2$$

in which n is purported to be characteristic of the surface roughness only. Substitution of equation (2.2) into equation (2.1) gives equation (2.3) which is known as the Manning flow resistance equation.

$$V = \frac{1}{n} R^{2/3} S^{1/2} \qquad 2.3$$

Equation (2.3) has been the most widely used resistance equation in practical river hydraulics. The Darcy-Weisbach equation (equation 2.4) is another widely used equation for pipes and channels. It was first proposed by Weisbach for pipes in 1845 and for channels in 1850.

$$V = \sqrt{\frac{8g}{f}} \sqrt{RS} \qquad 2.4$$

Equations (2.1), (2.3) and (2.4) are clearly similar in form and are interchangeable in practice, with obvious relationships between C, n and f (James et al., 2001). By convention, different equations are used in different circumstances and appropriate coefficients estimated in different ways (James et al., 2001).

These three flow resistance equations also assume steady uniform flow if S is taken as the bed slope, S_0. Steady uniform flow is a flow in open channel where the depth of flow does not change, or the flow can be assumed to be constant during the time interval under consideration (Chadwick and Morfett, 1993).

The resistance coefficient or friction factor can be related to the size of roughness elements on the bed, usually represented by the Nikuradse roughness k_s, and the Reynolds number (defined as $\mathrm{Re} = 4RV/v$), in which v is the kinematic viscosity (James et al., 2001). For laminar flow in pipes the friction factor depends on Reynolds number only, and not on the surface roughness (James et al., 2001)(equation (2.5)).

$$f = \frac{8g}{C^2} = \frac{64}{\mathrm{Re}} \qquad 2.5$$

For turbulent flow the relationship between f, C, Re and relative roughness is commonly expressed by equations (2.6), (2.7) and (2.8). The ASCE Task Force on Friction Factors in Open Channels (1963) reviewed the information available at the time and recommended using f rather than n because it correlates better with experimental data over a wide range of conditions.

For hydraulically rough flow:

$$\frac{1}{\sqrt{f}} = c \log\left(a \frac{R}{k_s} \right) \qquad 2.6$$

For hydraulically smooth flow:

$$\frac{1}{\sqrt{f}} = c \log\left(\mathrm{Re} \frac{\sqrt{f}}{b} \right) \qquad 2.7$$

For transitional flow:

$$\frac{1}{\sqrt{f}} = -c \log\left(\frac{k_s}{aR} + \frac{b}{\mathrm{Re}\sqrt{f}} \right) \qquad 2.8$$

The flow is hydraulically rough if the shear Reynolds number $\left(\mathrm{Re}_* = \frac{u_* k_s}{v} \right)$, where u_* the shear velocity is, exceeds 70 ($\mathrm{Re}_* > 70$). When the Reynolds number lies between 5 and 70 ($5 < \mathrm{Re}_* < 70$), the flow is transitional. The flow is hydraulically smooth if the shear Reynolds number is less than 5 ($\mathrm{Re}_* < 5$).

Equations (2.6), (2.7) and (2.8) are recommended for estimating f (ASCE Task Force on Friction Factors in Open Channels, 1963). The Task force presented values of the coefficients a, b and c derived from various data sets for rigid boundary channels. The representative values are:

$a = 12$

$b = 2.51$

$c = 2$

Values of k_s for concrete and masonry surfaces are tabulated in most open channel texts. These values range from 0.15 mm for very smooth concrete to 1.5 mm for gunite or shot concrete to greater than 5 mm for rubble masonry.

Equations (2.6) to (2.8) can also be used for unlined alluvial channels where bed forms are not present and resistance to flow arises from surface friction (James et al, 2001). It was also found that the appropriate value of k_s is determined by the grain size of the sediment, but as a range of sizes is usually present, specification of a representative value is not straightforward. Values recommended by various researchers in terms of grain size measures (D_i) are listed in Table 2.1.

Table 2.1: Recommended k_s values

Source	k_s
Ackers and White (1973)	$1.25\ D_{35}$
Hey (1979)	$3.5\ D_{84}$
Engelund and Hansen (1967)	$2\ D_{65}$
Kamphuis (1974)	$2.5\ D_{90}$
Mahmood (1971)	$5.1\ D_{84}$
Van Rijn (1982)	$3\ D_{90}$

Jordanova et al (2004) estimated the flow resistance of intermediate scale roughness by applying the following hypothesis:

- If the relative submergence is equal or bigger than four, then friction resistance dominates, and velocity can be estimated as

$$V = \frac{1}{n} R^{2/3} \sqrt{S} \qquad 2.9$$

- If the relative submergence is equal to or less than one, the drag effect of individual roughness elements on flow resistance will dominate and equation 2.10 should be used

$$V = \frac{1}{F}\sqrt{S} \qquad 2.10$$

where F is the resistance coefficient

- As the relative submergence increases from one to four, the dominant resisting effect changes gradually from element drag to friction. The velocity can be estimated by

$$V = a\frac{1}{F}\sqrt{S} + (1-a)\frac{1}{n}R^{2/3}\sqrt{S} \qquad 2.11$$

where a is coefficient related to the relative submergence. When the relative submergence is equal to one, the roughness is large scale. In this case $a = 1$ and equation (2.11) reduces to equation (2.10). When the relative submergence is four, the roughness is small scale, and a becomes 0 to reduce equation (2.11) to equation (2.9). Application of the proposed equation (2.11) required specification of the coefficient a as a function of the relative submergence.

A suitable relationship form was found to be the power function

$$a = b\left(\frac{y}{h}\right)^{c} \qquad 2.12$$

2.3. Roughness Characteristics

Characteristics of the roughness which most affect flow resistance are the size and shape of the roughness elements, the roughness concentration and the spacing between elements (Roberson and Wight., 1973). They further mentioned that only the roughness size is used in a direct way when determining a resistance coefficient. It was also mentioned by Bathurst (1978) that for real flows, the resistance to flow should be related to the size, shape, spacing and size distribution of the roughness elements and to channel geometry.

2.3.1. Roughness Size

A measure of the size is necessary for defining the relative submergence. The use of the equivalent sand roughness height, k_s to account for boundary resistance has been very useful for pipe flows (Vanoni and Brooks, 1957). They further stated that the concept is less useful for channels since k_s is not a measure of the actual roughness height but of the effect on the flow of that roughness determined experimentally.

2.3.2. Roughness Shape

When the water depth is similar to the size of the bed material, individual roughness elements protrude through the water surface and the flow resistance is caused by the form drag of the roughness elements and free surface distortion. Therefore understanding of the influence of the drag force on overall flow resistance is required. Experimental studies on the drag of hemispheres were conducted at Utah State University (Tullis, 1966). The results of the studies were used to identify the variables affecting the drag on a hemisphere for various flow conditions. Bathurst (1978) found that the shape of roughness elements affects the drag coefficient. The drag coefficient for the object is determined under the assumptions that there is a

uniform field of approach velocity and that the object is very long in the flow direction normal to that in which the transverse flow is made (Jordanova et al., 2004).

Furthermore it was found that in natural sediments, roughness shape is determined largely by the local geology, so in a region of given geology the effect of shape is likely to be constant (Bathurst, 2002). In 1982, Bathurst found from his experiments that the effect of roughness shape on the roughness parameter is limited. The relationship between roughness shape and resistance coefficient has not yet been delineated.

2.3.3. Roughness Size Distribution

The use of a single percentile of the size distribution requires that the ratio of that percentile to any other percentile should be constant from site to site (Bathurst, 1982). This condition can be tested using the standard deviation of the size distribution because natural sediments have size distributions which, while not exactly lognormal, are usually approximately to S_0 and the standard deviation depends on a ratio of percentiles.

As has been mentioned, for sediment with non-uniform size distribution, the ratio of approach to mean flow velocity and the drag varies from boulder to boulder (Bathurst, 1978).

2.3.4. Roughness Spacing

The spacing of roughness elements can influence flow resistance in open channels. When the roughness elements arranged in staggered pattern, the spacing of roughness elements has more influence on flow resistance. This is because the flow of water does not pass freely through the roughness elements. When the roughness elements arranged in parallel pattern, the spacing of roughness elements does not create more

resistance. This is because the flow of water moves freely through the roughness elements. The spacing of roughness elements that are close to each other creates more resistance than for those that are not close to each other.

CHAPTER 3: EXPERIMENTAL AND COMPUTATIONAL METHODS

3. Laboratory Experiments

Predicting the flow resistance of roughness elements is of great importance in hydraulics, because of their importance in practical application. Individual roughness elements within a natural channel vary in number, size, shape and distribution pattern. Thus a large number of variables affect resistance.

A series of experiments have been carried out to investigate the influence of size, spacing and arrangement of roughness elements on flow resistance.

3.1. Experimental Facilities

The experiments were conducted in the hydraulics laboratory at the University of the Witwatersrand. A rectangular glass-walled flume, 10 m long and 0.38 m wide was used to model a river channel (Fig. 3.1). The slope of the flume was 0.0047.



Figure 3.1: Tilting glass-walled flume

Flow was released from an elevated constant head tank to the flume. A vertical weir at the downstream end of the flume was adjusted in each experiment to ensure uniform flow. A pointer gauge was used to measure the flow depth. Discharge was controlled by a valve in the pipe between the overhead supply tank and the flume.

Discharge was measured by a v-notch weir installed in a sump at the downstream end of the flume and by an electronic flow meter in the supply pipe. For higher discharges (> 0.0243 m^3/s), the v-notch could not be used as water exiting the flume produced turbulence in the storage bay, making reading of v-notch measurements difficult and then only the electronic flow meter was used. The v-notch and flow meter reading agreed well for the lower flows.

3.2. Experimental Parameters

Other variables were kept constant in laboratory experimentation to determine the effect of one variable. The roughness of the flume (bed roughness), the cross-sectional shape, and the slope of the flume were kept constant for a specific set of experiments. The same shape of roughness elements (hemispherical) with different sizes was chosen to represent river rocks (Fig. 3.2). These hemispherical roughness elements were made of concrete with diameters of 112 mm, 72 mm and 46 mm.



Figure 3.2: Hemispherical roughness elements

The experiments were carried out with two patterns (staggered and parallel) as shown in Figs. 3.3 and 3.4. These figures illustrate the two patterns of roughness elements being modelled with equal spacing from centre to centre (a).

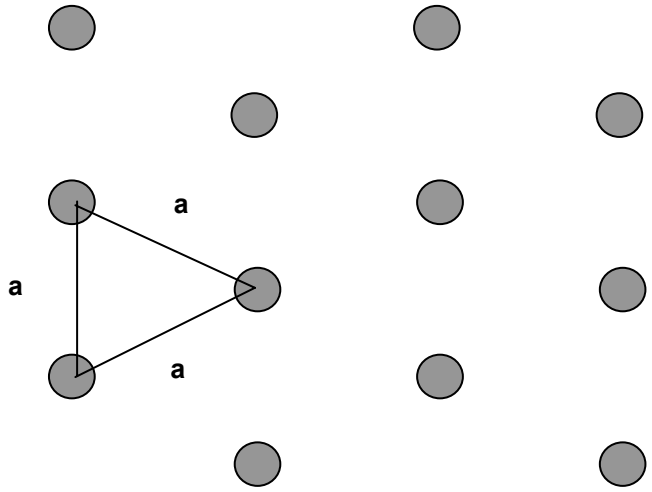


Figure 3.3: Staggered pattern

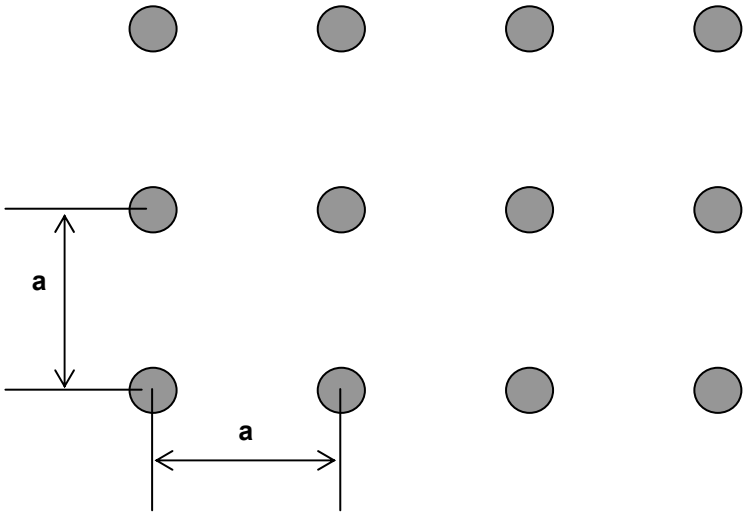


Figure 3.4: Parallel pattern

3.3. Experimental Procedure

All experiments were carried out under uniform flow conditions. The two roughness patterns (staggered and parallel) were created within the tilting glass-walled flume using hemispheres with diameters of 112 mm, 72 mm and 46 mm (Figs. 3.3 and 3.4). A tailgate at the downstream end of the flume was used to control the flow depth in the channel to ensure uniform flow. The velocity of flow was calculated from the experimental data listed in Appendix A (Table A.1 – A.3). The following procedure was applied to establish uniform flow:

- Water was released from an elevated constant head tank to the flume.
- The position of the vertical weir was set at an arbitrary level and the water level allowed to reach equilibrium.
- The discharge was varied by adjusting (opening/closing) the control valves and measured using V-notch, which is installed at the downstream end of the flume, and an electronic flow meter with sensors that are situated in the water pipe that discharges into the flume.
- Once the uniform flow was reached, the bed level and water surface were measured in order to get the mean flow depth.

3.4. Test Series Description

The experimental study included four test series (Series A, B, C and D). The first set of experiments (Series A experiments) was conducted in an empty flume to establish its roughness. Series B, C and D experiments included particular roughness size and each including three to seven runs with different discharges and roughness densities (see Table 3.1).

Series B and C experiments were conducted with hemispheres with diameters of 112 mm and 72 mm respectively arranged in staggered and parallel patterns, to investigate

the effect of roughness element pattern and spacing on flow resistance. Further details of experimental conditions of experimental series A, B, C and D are described in the sub-sections 3.4.1, 3.4.2, 3.4.3 and 3.4.4 below.

3.4.1. Series A Experiments

This series comprised three experiments in the empty flume to establish the roughness of an empty flume (Test 1, Table 3.1).

3.4.2. Series B Experiments

Series B experiments were carried out using hemispheres with a diameter of 112 mm, to investigate the effect of roughness element pattern and density on flow resistance. The hemispheres were arranged in staggered (Tests 2 and 3, Table 3.1) and parallel (Test 4, Table 3.1) patterns. The experiments were preformed for three densities, and centre to centre spacing for each test is given in Table 3.1.

3.4.3. Series C Experiments

Series C experiments were carried out using hemispheres with a diameter of 72 mm, to investigate the effect of roughness element spacing and density on flow resistance. The hemispheres were arranged in parallel (Tests 5 and 8, Table 3.1) and staggered (Tests 6 and 7, Table 3.1) patterns. The experiments were performed for four densities, and centre to centre spacing for each test is given in Table 3.1.

3.4.4. Series D Experiments

This series was carried out using hemispheres with diameter of 46 mm, to establish the flow resistance of the bed for roughness elements with diameter of 46 mm. The

hemispheres were arranged in staggered pattern (Test 9, Table 3.1). Only one pattern and one density were investigated.

Table 3.1: Experimental Conditions for Series A, B, C and D Experiments

Series	Test	Number of Runs	Q (m^3/s)	y (m)	AC (%)	D (mm)	h (mm)	a (mm)	No./m	Pattern
A	1	3	0.0241 - 0.0379	0.0715 - 0.1135	0	-	-	-	-	-
B	2	7	0.0044 - 0.0546	0.0865 - 0.2585	62	112	56	134	24	Staggered
	3	6	0.0011 - 0.0552	0.0540 - 0.2555	30	112	56	177	12	Staggered
	4	5	0.0026 - 0.0427	0.0575 - 0.2005	26	112	56	190	10	Parallel
C	5	5	0.0027 - 0.0430	0.0350 - 0.1635	11	72	36	190	10	Parallel
	6	5	0.0027 - 0.0422	0.0360 - 0.1630	15	72	36	177	14	Staggered
	7	5	0.0060 - 0.0421	0.0747 - 0.2030	29	72	36	123	27	Staggered
	8	6	0.0026 - 0.0498	0.0515 - 0.2320	64	72	36	77	60	Parallel
D	9	4	0.0026 - 0.0260	0.0310 - 0.1030	6	46	23	177	14	Staggered

AC = area coverage, D = diameter of hemispheres, h = height of hemispheres, a = spacing of hemispheres, No./m = number of hemispheres per meter flume of length, y = flow depth.

3.5. Side -Wall Correction Procedure

The flume is narrow relative to the flow depth and the bed of the flume is rougher than the side walls. Therefore the side wall correction procedure of the Vanoni and Brooks (1957) was applied to determine the friction of the bed(f_b). The method depends on the following relationships:

$$\frac{\mathrm{Re}}{f} = \frac{\mathrm{Re}_w}{f_w} = \frac{\mathrm{Re}_b}{f_b} \qquad 3.1$$

and

$$\frac{R}{f} = \frac{R_w}{f_w} = \frac{R_b}{f_b} \qquad 3.2$$

where Re the Reynolds number of the channel is, f is the friction factor of the channel and the subscripts w and b refer to the wall and bed respectively. The Reynolds number of the wall (Re_w) may be rearranged as follows:

$$\mathrm{Re}_w = \frac{4U_w R_w}{\nu}, \frac{4U_w R_f}{\nu}\frac{R_w}{R_f} = \mathrm{Re}_f \frac{R_w}{R_f} \qquad 3.3$$

where U is the depth average velocity and Re_f is the Reynold number of the friction.

The procedure used for estimating bed characteristics is as follows:

1. Calculate Re and f for the whole cross-section (from experimental data) and compute Re_w/f_w, which is equal to Re/f according to equation 4.1.

2. Plot $\mathrm{Re}_w/f_w = \mathrm{Re}/f$ = constant on the friction factor diagram (Brownlie, 1981) as a straight line with a slope of 1 in log units, and with the intercept at $f = 0.01$ at $0.01\,\mathrm{Re}/f$.
3. Select a trial value of R_w, compute $4R_w/k_{sw}$ (where k_{sw} is the effective roughness of the wall), and determine f_w from friction factor diagram (Brownlie, 1981).
4. Compute $R_w = \left(\frac{R}{f}\right) f_w$ and compare with the selected value. Iterate to convergence.
5. Calculate f_b and R_b from equations 4.2 and

$$p_f = p_b f_b + p_w f_w \qquad 3.4$$

In this application k_{sw} is not known and the procedure was carried out the other way round, using a trial value of R_b and following the procedure from step 3 to produce values for f_w and R_w.

The corresponding values of Manning's n for the wall and bed were calculated by equating the Manning's n and Darcy-Weisbach formula to give:

$$n_w = R_w^{1/6}\left(\frac{f_w}{8g}\right)^{1/2} \qquad 3.5$$

$$n_b = R_b^{1/6}\left(\frac{f_b}{8g}\right)^{1/2} \qquad 3.6$$

The subscripts w in equation (3.2) and b in equation (3.3) refer to the wall and bed of the channel respectively.

The use of Manning's n helps to interpret the influence of roughness elements size, shape and arrangement on flow resistance. The effective roughness of the bed (k_s) has also been calculated from Colebrook-White transition equation (3.8).

3.6. The Effective Roughness of the bed

The effective roughness of the bed (k_s) was calculated by rearranging the Colebrook-White transition formula, i.e.

$$\frac{1}{\sqrt{f}} = -2\log\left(\frac{k_s}{12R} + \frac{2.51}{\mathrm{Re}\sqrt{f}}\right) \qquad 3.7$$

to give

$$k_s = 12R\left(\frac{1}{10^{-2\sqrt{f}}} - \frac{2.51}{\mathrm{Re}\sqrt{f}}\right) \qquad 3.8$$

The effective roughness of the bed (k_s) is very important in determining the friction factor of a bed in open channel. Additionally, assessment of the effect of roughness elements on flow resistance requires knowledge of the resistance characteristics of the bed, so that the effects can be separated and that the bed can be represented correctly (James et al, 2001). The results of the analysis are presented in Tables 4.1 – 4.9.

CHAPTER 4: RESULTS AND DISCUSSION

4.1. Experimental Results

The flow resistance was expressed and presented in terms of Manning's n, because it is the most common and widely used formula for open channel flow. The values for Manning's n and velocity were calculated from the experimental data listed in Appendix A (Tables A.1 – A.3). The calculated and predicted velocities were also computed from the experimental data given in Appendix B (Table B.1).

4.1.1. Series A Experimental Results

The analysis of the results for friction factors of the bed are shown in Table 4.1.

Table 4.1: Hydraulic Parameters and Friction Factors of the Bed for Series A

Q (m^3/s)	0.02454	0.0376	0.0461
y (m)	0.0715	0.0907	0.1135
S	0.0047	0.0047	0.0047
R_f (m)	0.0520	0.0614	0.0711
R_b (m)	0.0522	0.0679	0.0846
f_b	0.0220	0.0210	0.0273
Re_b	48838	74079	90464
n_b	0.0126	0.0133	0.0116

where: R_f = hydraulic radius (flume),

R_b = hydraulic radius (bed),

f_b = friction factor (bed),

Re_b = Reynolds number (bed),

n_b = Manning's (bed), and

y = Flow depth.

4.1.2. Series B Experimental Results

Series B experiments comprised three tests (Tests 2, 3 and 4) with the same size of roughness elements (112 mm), each with different densities and center to center spacing. Tests 2 and 3 were arranged in the same pattern (staggered), but with different area coverage and spacing (Table 3.1). Tests 3 and 4 were arranged in different patterns (staggered for Test 3 and parallel for Test 4) and spacing, but with almost the same spacing and area coverage (Table 3.1). Test 2 and 4 were arranged in different patterns (staggered for Test 2), spacing and area coverage.

Table 4.2: Hydraulic Parameters and Friction Factors of the Bed for Test 2

Q (m^3/s)	0.0047	0.0056	0.0134	0.0197	0.0376	0.0479	0.0546
y (m)	0.0865	0.0905	0.1330	0.1520	0.2095	0.2455	0.2585
S	0.0047	0.0047	0.0047	0.0047	0.0047	0.0047	0.0047
R_f (m)	0.0594	0.0613	0.0782	0.0844	0.0996	0.1071	0.1095
R_b (m)	0.0852	0.0889	0.1284	0.1446	0.1936	0.2244	0.2339
f_b	1.5377	1.2369	0.6736	0.4585	0.3202	0.3140	0.2792
Re_b	12188	14479	34039	49312	91452	115241	130002
n_b	0.0930	0.0840	0.0659	0.0554	0.0486	0.0494	0.0469

Table 4.3: Hydraulic parameter values and friction factor of the bed for Test 3

Q (m^3/s)	0.0011	0.0065	0.0229	0.0413	0.0489	0.0552
y (m)	0.0540	0.1025	0.1520	0.2155	0.2340	0.2555
S	0.0047	0.0047	0.0047	0.0047	0.0047	0.0047
R_f (m)	0.0420	0.0666	0.0844	0.1010	0.1049	0.1090
R_b (m)	0.0538	0.1007	0.1430	0.1995	0.2170	0.2362
f_b	6.9057	1.3332	0.3356	0.2894	0.2647	0.2695
Re_b	2884	16797	56695	100637	119355	134275
n_b	0.1826	0.0890	0.0473	0.0465	0.0451	0.0461
k_s	0.4164	0.4455	0.2350	0.2816	0.2778	0.3084

Table 4.4: Hydraulic Parameter Values and Friction Factor of the Bed for Test 4

Q (m^3/s)	0.0030	0.0076	0.0195	0.0315	0.04334
y (m)	0.0575	0.0765	0.1150	0.1640	0.2005
S	0.0047	0.0047	0.0047	0.0047	0.0047
R_f (m)	0.0441	0.0545	0.0716	0.0880	0.0976
R_b (m)	0.0342	0.0617	0.0807	0.1133	0.1429
f_b	1.1092	0.4027	0.1980	0.2205	0.2013
Re_b	7783	19508	47700	77214	100885
n_b	0.0738	0.0466	0.0347	0.0388	0.0380
k_s	0.2278	0.1457	0.0964	0.1578	0.1632

4.1.3. Series C Experimental Results

Series C experiments comprised four tests (Tests 5, 6, 7 and 8) with the same size of roughness elements (72 mm), but with different spacing. Tests 5, 6 and 7 have the different densities to that of Test 8. Tests 5 and 8 were arranged in the same pattern (parallel), but with different area coverage (Table 3.1). Tests 6 and 7 were arranged in the same pattern (staggered), but with different area coverage (Table 3.1).

The results for Test 5 were compared to Test 8 to investigate the influence of roughness element spacing on flow resistance (Fig 4.4).

The results of the analysis of the friction factor of the bed are shown in Tables (4.5 to 4.8).

Table 4.5: Hydraulic Parameter values and Friction Factor of the Bed for Test 5

Q (m^3/s)	0.0027	0.0083	0.0197	0.0304	0.0430
y (m)	0.0350	0.0650	0.0910	0.1255	0.1635
S	0.0047	0.0047	0.0047	0.0047	0.0047
R_f (m)	0.0296	0.0484	0.0615	0.0756	0.0879
R_b (m)	0.0342	0.0617	0.0807	0.1133	0.1429
f_b	0.3058	0.2017	0.0917	0.1028	0.1101
Re_b	6936	20744	45984	72207	98927
n_b	0.0356	0.0319	0.0225	0.0252	0.0271
k_s	0.0508	0.0569	0.0215	0.0374	0.0532

Table 4.6: Hydraulic Parameter values and Friction Factor of the Bed for Test 6

Q (m^3/s)	0.0027	0.0075	0.0181	0.0283	0.0430
y (m)	0.0360	0.0665	0.1015	0.1360	0.1630
S	0.0047	0.0047	0.0047	0.0047	0.0047
R_f (m)	0.0303	0.0493	0.0662	0.0793	0.0877
R_b (m)	0.0352	0.0644	0.0937	0.1260	0.1433
f_b	0.0.3331	0.2695	0.1570	0.1550	0.1097
Re_b	6942	19102	43980	68993	99462
n_b	0.0374	0.0372	0.0302	0.0315	0.0271
k_s	0.0571	0.0839	0.0614	0.0810	0.0530

Table 4.7: Hydraulic Parameters and Friction Factors of the Bed for Test 7

Q (m^3/s)	0.0060	0.0147	0.0238	0.0322	0.0421
y (m)	0.0745	0.1160	0.1475	0.1740	0.2030
S	0.0047	0.0047	0.0047	0.0047	0.0047
R_f (m)	0.0535	0.0720	0.0830	0.0908	0.0981
R_b (m)	0.0730	0.1101	0.1378	0.1615	0.1882
f_b	0.5994	0.3652	0.2819	0.2512	0.2330
Re_b	15470	36720	58507	78658	102691
n_b	0.0566	0.0473	0.0431	0.0418	0.0413

Table 4.8: Hydraulic Parameters and Friction factors of the Bed for Test 8

Q (m^3/s)	0.0026	0.0064	0.0138	0.0280	0.0448	0.0498
y (m)	0.0515	0.0758	0.1140	0.1655	0.2155	0.2320
S	0.0047	0.0047	0.0047	0.0047	0.0047	0.0047
R_f (m)	0.0405	0.0542	0.0713	0.0885	0.1010	0.1045
R_b (m)	0.0189	0.0275	0.0386	0.0497	0.0661	0.0708
f_b	1.0620	0.5498	0.3973	0.2834	0.2461	0.2482
Re_b	6752	16350	34822	67807	109235	121267
n_b	0.0709	0.0543	0.0493	0.0440	0.0429	0.0436
k_s	0.1993	0.1867	0.2110	0.2101	0.2352	0.2553

4.1.4. Series D Experimental Results

As mentioned in section 3.4.4, series D experiments were carried out with one roughness elements size (46 mm) and one density, to establish its flow resistance. These experiments were arranged only in staggered pattern (Test 9, Table 3.1). The results of the analysis of the friction factor of the bed are shown in Table 4.9.

Table 4.9: Hydraulic Parameters and Friction Factors of the Bed for Test 9

Q (m^3/s)	0.0026	0.0115	0.0154	0.0260
y (m)	0.0310	0.0755	0.0790	0.1030
S	0.0047	0.0047	0.0047	0.0047
R_f (m)	0.0267	0.0540	0.0558	0.0668
R_b (m)	0.0304	0.0712	0.0734	0.0880
f_b	0.2298	0.1635	0.1029	0.0735
Re_b	6699	28543	37665	58426
n_b	0.0303	0.0294	0.0235	0.0204
k_s	0.0327	0.0494	0.0149	0.0242

4.2. Influence of Roughness Element Size on Flow Resistance

The roughness elements with different sizes were conducted with the same area coverage and pattern to investigate the size effect on flow resistance.

The results for Test 3 (112 mm) were compared with Test 7 (72 mm) to investigate the effect of roughness element size on flow resistance (Fig. 4.1). The results of Test 3 were also compared with Test 4 to investigate the effect of roughness element pattern on flow resistance (Fig. 4.5).

The analysis of the results for friction factor of the bed for Tests 3 and 7 is given in Tables 4.3 and 4.7 respectively. The analysis of the results for friction factor of the bed for Tests 2 and 4 is given in Tables 4.2 and 4.4 respectively.

The effect of roughness element size on flow resistance in terms of Manning's n with the relative submergence is presented in Fig. 4.1. Results suggest that resistance is influenced by the size of roughness element. It can be noted from Fig. 4.1 that Manning's n for Test 7 is higher than that of Test 3. This means that Manning's n varies with relative submergence much more for small size of roughness elements than for large size of roughness elements.

The upper transitional limit for Test 3 occurs at a relative submergence of about 3 below which the values of Manning's n increase with decreasing relative submergence. At a relative submergence of about 4, Test 3 shows that above this level the size of roughness element has no significant effect on flow resistance (Fig. 4.1).

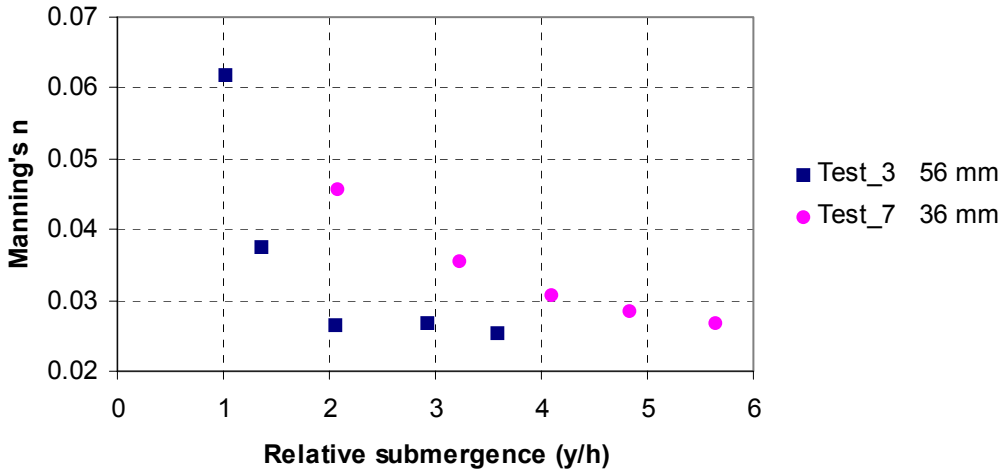


Figure 4.1: Effect of roughness element size on flow resistance

The hydraulic parameters and bed friction factor for Tests 3 and 7 are shown in Tables 4.3 and 4.7 respectively. The friction factor of the bed, f_b was plotted against flow depth in Fig 4.2.

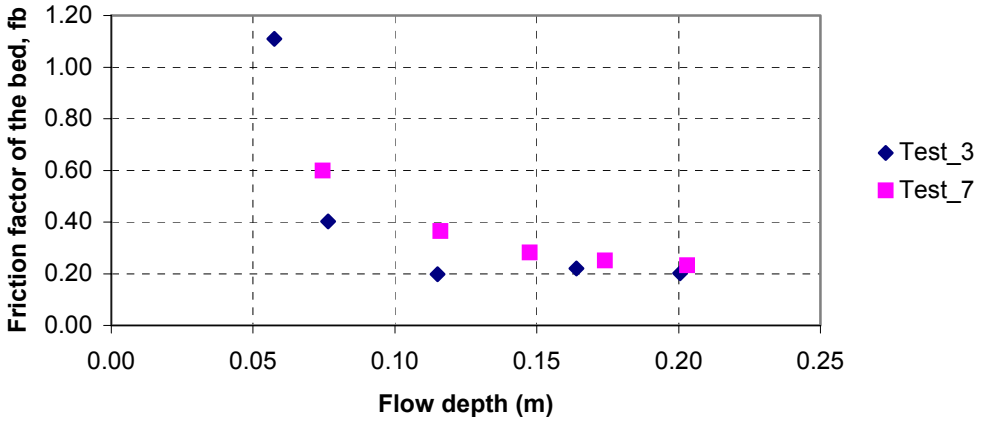


Figure 4.2: Friction factor of the bed vs. Flow depth

It can be noted from Fig. 4.2 that the friction factor of the bed for Test 7 was higher than that of Test 3. This means that the friction factor of the bed varies with relative submergence much more for small size of roughness elements than for large size of roughness elements.

4.3. Influence of Roughness Element Spacing on Flow Resistance

The spacing of roughness elements in flow resistance is important since it has resulted into good correlation (correlation 4, equations 5.9 and 5.10) that has contributed to the proposed equation (5.13). This equation (5.13) worked well when tested to the experimental data performed by Jordanova (in preparation, Table 5.5).

It was found from the experimental data listed in Appendix A (Table A.1 – A.3) that the spacing of roughness elements arranged in parallel pattern with bigger area coverage (Test 8, Table 3.1) has more influence than that with smaller coverage area (Test 5, Table 3.1).

A comparison between Tests 5 and 8 showed that the roughness elements with smaller spacing has more effect on flow resistance that those with bigger spacing

(Fig. 4.3). It was also observed from the experimental study that the spacing of roughness elements arranged in staggered pattern (Fig. 3.3) has more influence on flow resistance than those arranged in parallel pattern (Fig. 3.4).

Tests 5 (hemispheres with 72 mm diameter) and 8 (hemispheres with 72 mm diameter) were carried out with the same bed slope and pattern, but with different spacing to investigate the spacing effect on flow resistance. The effect of roughness element spacing on flow resistance is shown in Fig. 4.3.

It can be noted from Fig. 4.3 that Manning's n varies with relative submergence for both Tests 5 and 8. The upper limit of transition zone is at relative submergence of about 3 for Test 5 and about 5 for Test 8. It can also be noted from Fig. 4.3 that the spacing for Test 8 is bigger than that of Test 5. This means that the flow resistance of the bed varies with flow depth much more for roughness elements with smaller spacing than those with larger spacing.

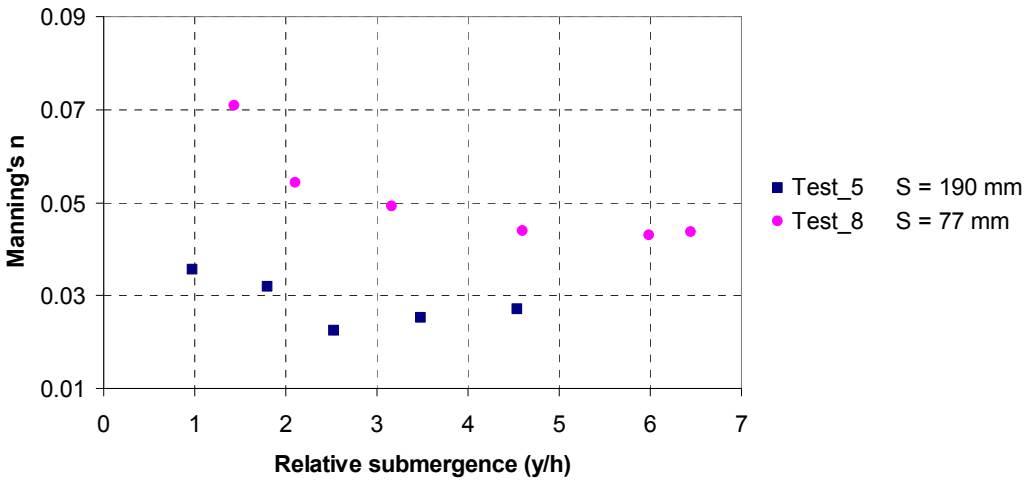


Figure 4.3: Effect of roughness element spacing on flow resistance

The hydraulic parameters and friction factors of the bed for Tests 5 and 8 are given in Tables 4.5 and 4.8 respectively. These tables also indicate the calculated effective

roughness of the bed (k_s). The friction factor of the bed has been plotted against flow depth in Fig. 4.4.

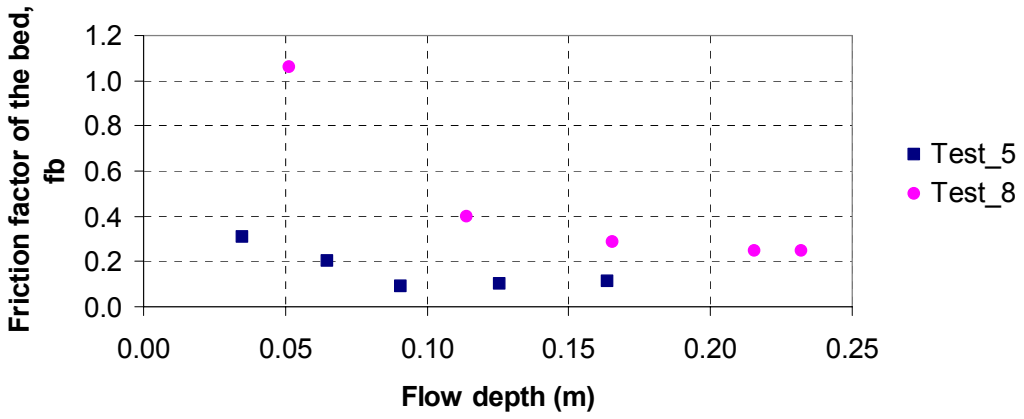


Figure 4.4: Friction factor of the bed vs. Flow depth

The friction factors of the bed for Test 8 was higher than that of Test 5. This suggests that the spacing of roughness elements has an effect on flow resistance, when the same size of roughness elements are arranged in the same pattern, but with different spacing (Fig. 4.4). This confirms that the roughness elements with smaller spacing has more effect on flow resistance that those with larger spacing.

4.4. Influence of Roughness Element Pattern on Flow Resistance

Tests 3 (hemispheres with 112 mm diameter) and 4 (hemispheres with 112 mm diameter) were conducted with the same size and almost the same area coverage, but with different pattern to investigate the effect of pattern on flow resistance. The pattern effect was investigated by plotting a graph of Manning's n with a relative submergence (Fig. 4.5).

It is clear from Fig. 4.5 that Manning's n for Tests 3 and 4 varies with relative submergence at in low flow condition. The Manning's n becomes constant at a

relative submergence value of about 3. This suggests that Manning's n depends on the pattern of roughness elements.

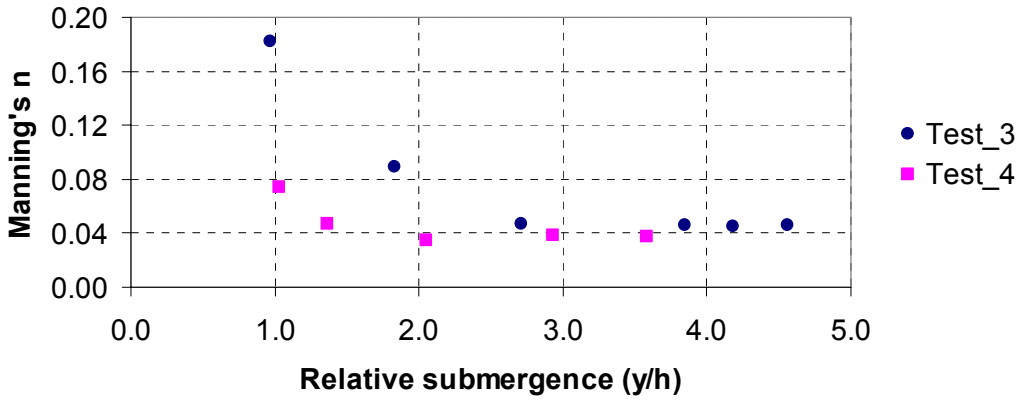


Figure 4.5: Effect of roughness element pattern on flow resistance

The hydraulic parameters and friction factors of the bed for Tests 3 and 4 are given in Tables 4.3 and 4.4 respectively. The friction factor of the bed has been plotted against flow depth in Fig. 4.6.

Figure 4.6 clearly indicates that the friction factor of the bed for Test 3 was higher than that for Test 4. But Tests 3 and 4 becomes constant at flow depth value of about 0.15. This means that staggered pattern affects flow resistance much more than parallel pattern.

This also suggests that the roughness element arranged in different pattern, but with almost the same area coverage have effect on flow resistance.

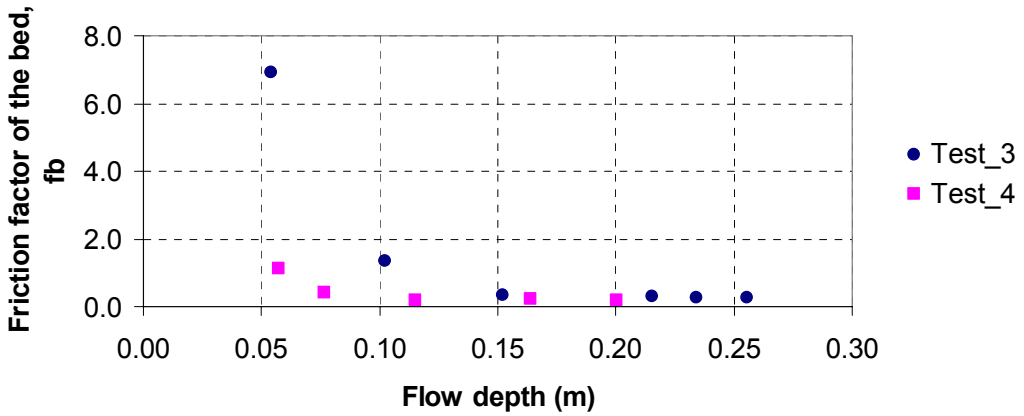


Figure 4.6: Friction factor of the bed vs. Flow depth

4.5. Conclusion

The laboratory experiments of flow resistance in open channels with intermediate roughness elements were carried out to investigate the influence of roughness element size, roughness element spacing and roughness element pattern. The results of the experiments showed that flow resistance expressed by Manning's n varies with flow condition. It was also found that resistance depends on roughness element size, roughness element spacing and roughness element pattern.

The values of friction factors of the bed was calculated using the side-wall correction procedure of Vanoni and Brooks (1957). These values showed that the roughness element size, roughness element spacing and roughness element pattern have significant influence on flow resistance.

CHAPTER 5: ANALYSIS AND PREDICTIVE RESULTS

5. Analysis and Predictive Results

This chapter presents the development of an equation for predicting Manning's n under intermediate scale roughness conditions. This was done by describing the variation of n with relative submergence by a power function and then correlating the parameters in this function with the different roughness characteristics. The proposed equation was verified by applied to a data set obtained from another study.

5.1. Flow Resistance Prediction

5.1.1. Flow Resistance of Small-Scale Roughness

When comparing the relative roughness to a Strickler function, it was found that over a wide range of relative roughness, the variation of the Strickler function is small (Chow, 1959). Because of this relationship, a constant value for the Strickler function can be used to calculate an n value.

The results for small-scale roughness conditions were compared to Strickler's equation (5.1) for n in terms of k_s to investigate the effect of size, pattern and spacing on this prediction. This equation was taken from the Water Research Commission Report No. 856/1/01 (James et al, 2001). A comparison with this experimental data included all the values of Manning's n for each element size. The values of Manning's n are different because the experimental study included four test series, each for a particular roughness size and each included three to seven runs with different discharges and roughness densities (Table 3.1).

The Manning's n values were plotted against the effective surface roughness height in Fig. 5.1. The effective surface roughness height in Fig. 5.1 is the height of the used hemispherical roughness elements with diameters of 46 mm, 72 mm and 112 mm.

$$n = \frac{k_s^{1/6}}{7.7 g^{1/2}} \qquad 5.1$$

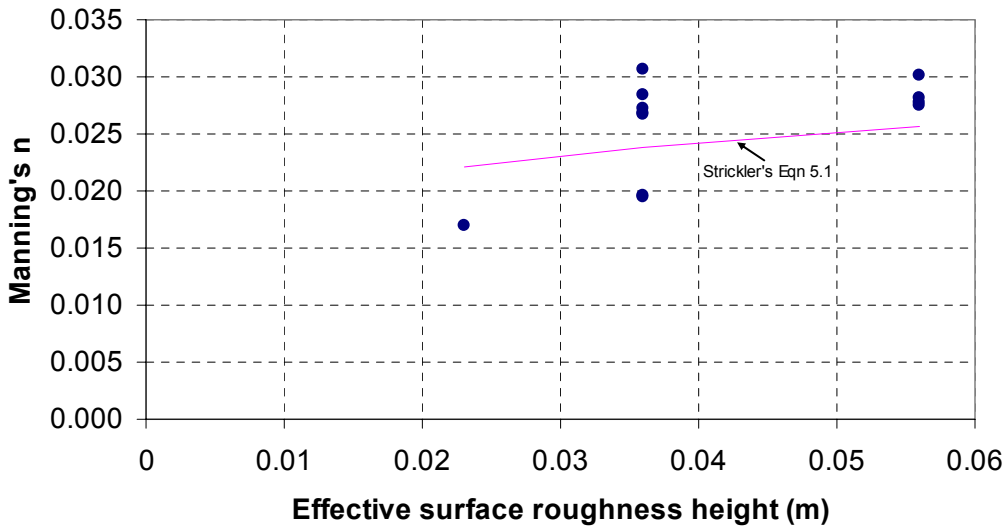


Figure 5.1: Manning's n vs. Effective surface roughness height

The n values predicted with the Strickler's equation are slightly lower than experimental values of the Manning's except for Tests 5, 6 and 9 (Table 5.1). Table 5.1 shows n values calculated by the Manning's and Strickler's equations. The values of Manning's n are also given in Appendix A (Tables A.1 to A.3).

Table 5.1: Manning's and Strickler's n values

Test	k_s (m)	n	n_s
2	0.056	0.0379	0.0256
3	0.056	0.0226	0.0256
4	0.056	0.0129	0.0256
5	0.056	0.0180	0.0256
6	0.036	0.0295	0.0238
7	0.036	0.0397	0.0238
8	0.036	0.0418	0.0238
9	0.023	0.0202	0.0221

where n_s is the Strickler's n value

The Manning's n for roughness elements with diameter of 46 mm (Test 9) is close to Strickler's equation (Table 5.1). Some Manning's n values for roughness elements with diameters of 72 mm (Test 8) and 112 mm (Tests 2 and 3) are close to each other and close to the Strickler's equation (5.1), whereas others are not close to each other (Tests 7 and 8, Tests 2 and 3) but close to Strickler's equation (5.1).

This shows that the Strickler's equation can be used to predict the n values for roughness elements with diameters of 46 mm, 72 mm and 112 mm (Table 5.1) as well as for the experiments conducted in an empty flume. The Manning's n values that are not close to each other indicate that the density of roughness element has a significant influence on flow resistance.

5.1.2. Flow Resistance of Intermediate-Scale Roughness

Flow resistance of intermediate-scale roughness was investigated to come up with an equation to be used under such condition. The resistance coefficient n was plotted against the relative submergence from the laboratory results.

A suitable form of the relationship was found to be the power function (equation 5.2; Figs 5.2 – 5.9).

$$n = a\left(\frac{y}{h}\right)^{b} \qquad 5.2$$

The plotted data was fitted with curves in Figs. 5.2 to 5.9 for the different experimental conditions. Only the intermediate-scale condition data were used to fit the curves shown in Figures 5.2 to 5.9.

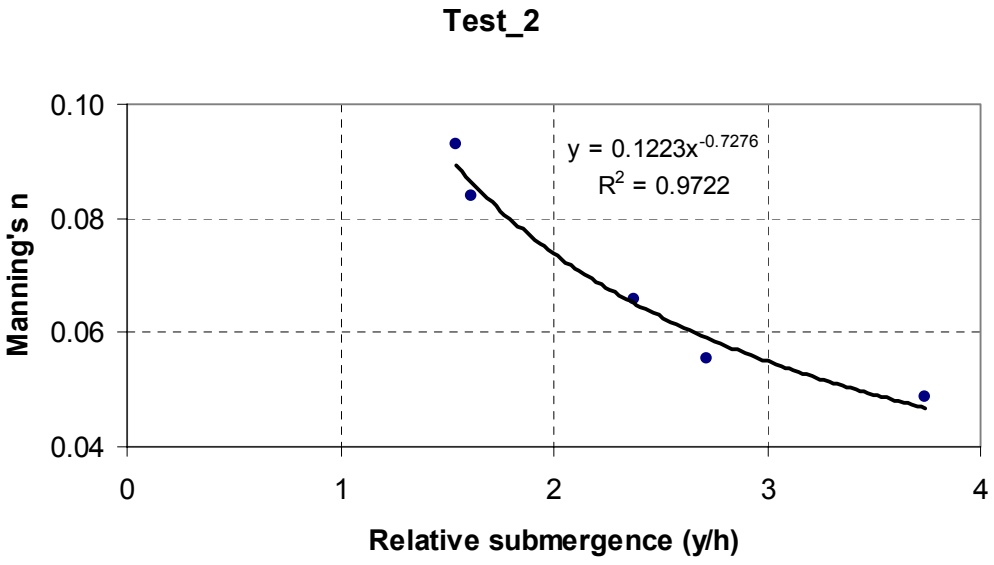


Figure 5.2: Manning's n vs. Relative submergence

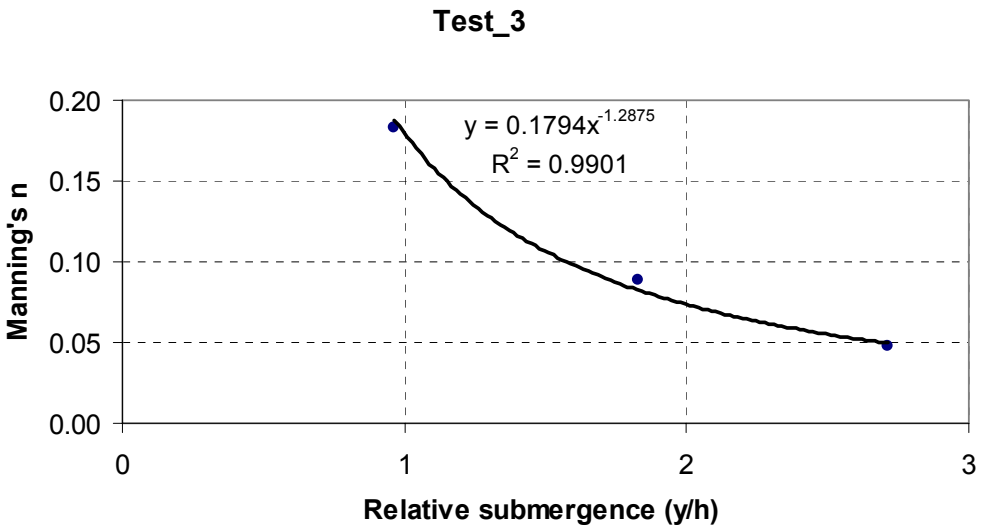


Figure 5.3: Manning's n vs. Relative submergence

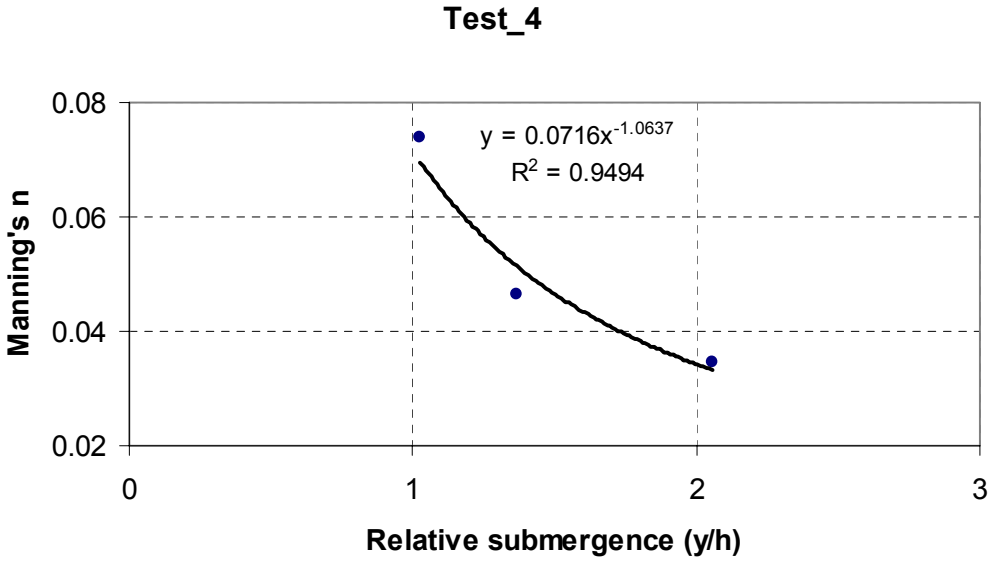


Figure 5.4: Manning's n vs. Relative submergence

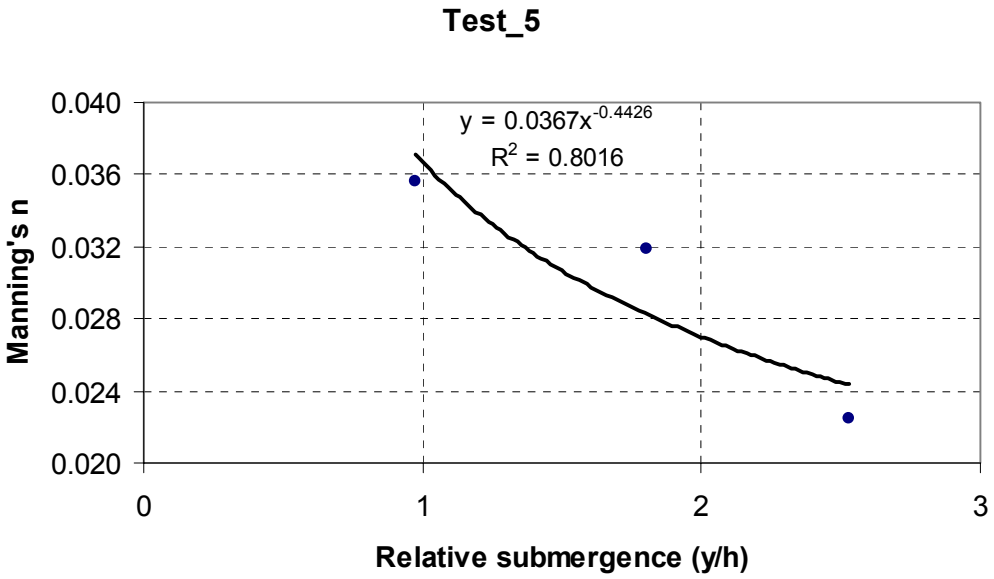


Figure 5.5: Manning's n vs. Relative submergence

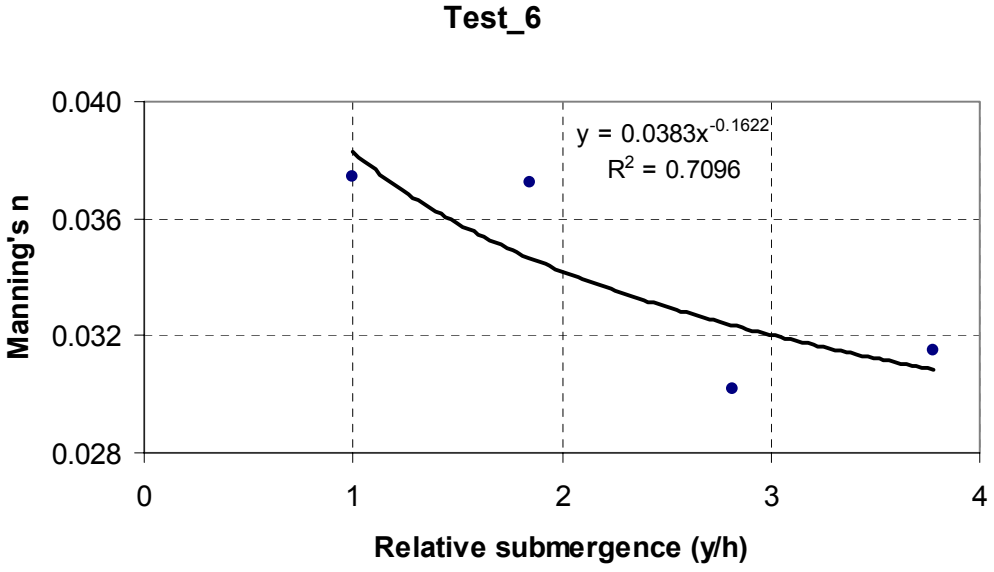


Figure 5.6: Manning's n vs. Relative submergence

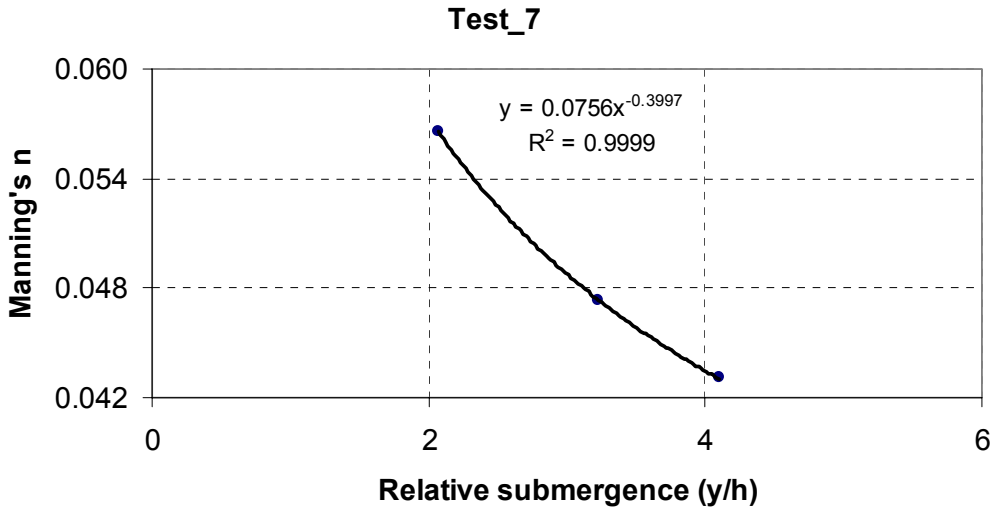


Figure 5.7: Manning's n vs. Relative submergence

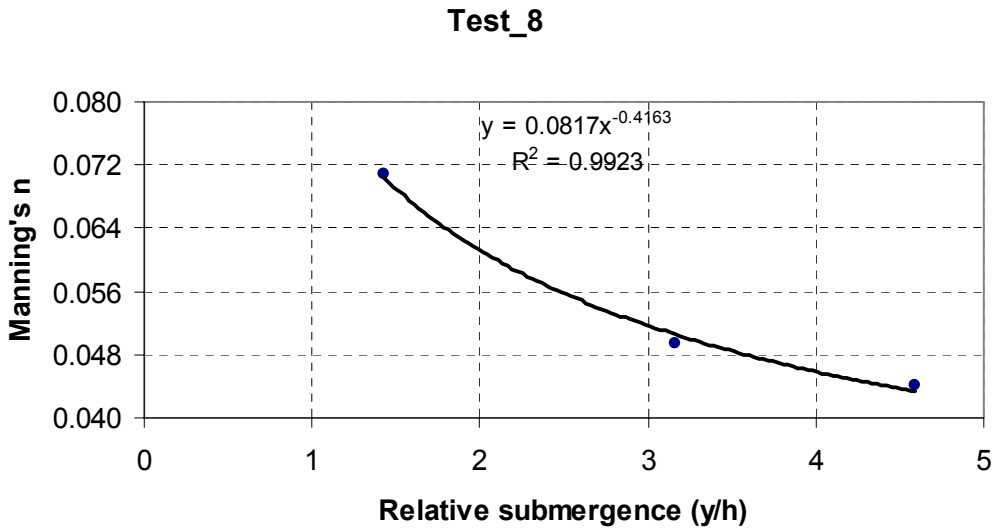


Figure 5.8: Manning's n vs. Relative submergence

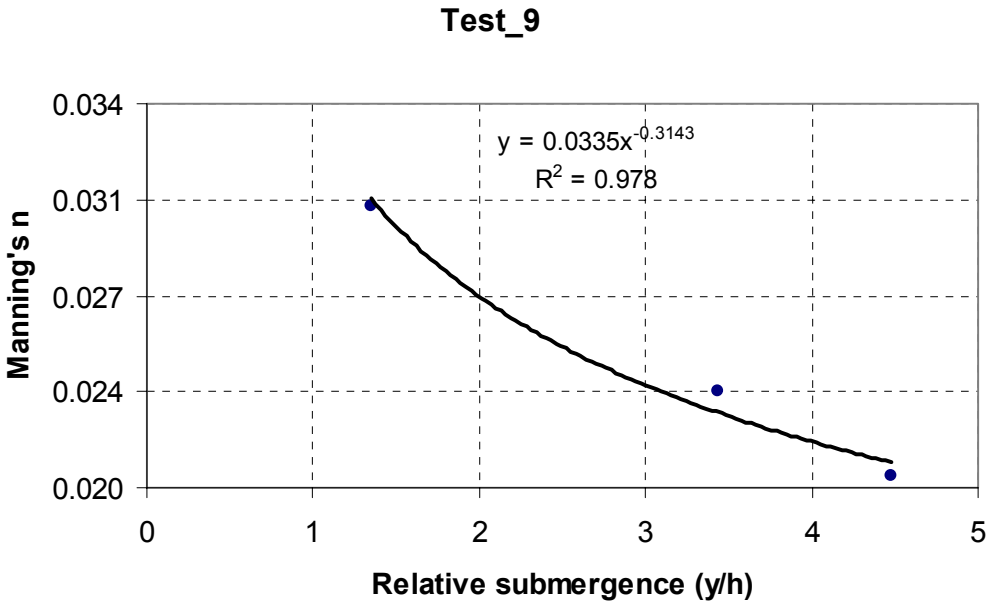


Figure 5.9: Manning's n vs. Relative submergence

5.2. Verification of Proposed Equation

The values of coefficient a and b were determined from Figs 5.2 to 5.9 and are given in Table 5.2. It can be seen from Table 5.2 that values for these coefficients are different for the fitted plotted curves. Therefore all the values for coefficients a and b were grouped together and plotted against different variables to come up with the best correlation.

Table 5.2: Values of Coefficients a and b for the different condition

Test	D (mm)	Sp (mm)	D/Sp	a	b	R^2- value
2	112	134	0.8358	0.1223	-0.7276	0.9722
3	112	177	0.6328	0.1798	-1.2875	0.9901
4	112	190	0.5895	0.0716	-1.0637	0.9494
5	72	190	0.3789	0.0367	-0.4426	0.8016
6	72	177	0.4068	0.0383	-0.1622	0.7096
7	72	123	0.5854	0.0756	-0.3997	0.9999
8	72	77	0.9351	0.0817	-0.4163	0.9923
9	46	177	0.2599	0.0335	-0.3143	0.9780

The following correlations (5.3 to 5.10) were done and compared to each other to come up with the best correlation. These correlations were based on the area coverage (AC), diameter (D) and ratio of diameter to spacing $\left(\frac{D}{Sp}\right)$ of roughness elements.

1. $$a = f\left(\frac{D}{Sp}\right) \quad 5.3$$

$$b = f(AC) \quad 5.4$$

2. $$a = f\left(\frac{D}{Sp}\right) \quad 5.5$$

$$b = f\left(\frac{D}{Sp}\right) \quad 5.6$$

3. $a = f(AC)$ 5.7

$b = f(AC)$ 5.8

4. $a = f\left(\frac{D}{Sp}\right)$ 5.9

$b = f(D)$ 5.10

Correlation 4 (i.e. equations 5.9 and 5.10) worked well because the r^2 values for this correlation is higher than those for correlations 1, 2, and 3 (see Figs. 5.10 and 5.14). A suitable form of relationship for coefficient a was therefore found to be the power function (Fig. 5.10).

$$a = 0.113\left(\frac{D}{Sp}\right)^{0.999} \quad 5.11$$

The suitable relationship for coefficient b was found to be a linear function (Fig. 5.14).

$$b = -0.012(D) + 0.376 \quad 5.12$$

Equations (5.11) and (5.12) were substituted into equation (5.2) to yield equation 5.13.

$$n = 0.113\left(\frac{D}{Sp}\right)^{0.999}\left(\frac{y}{h}\right)^{-0.012(D)+0.376} \quad 5.13$$

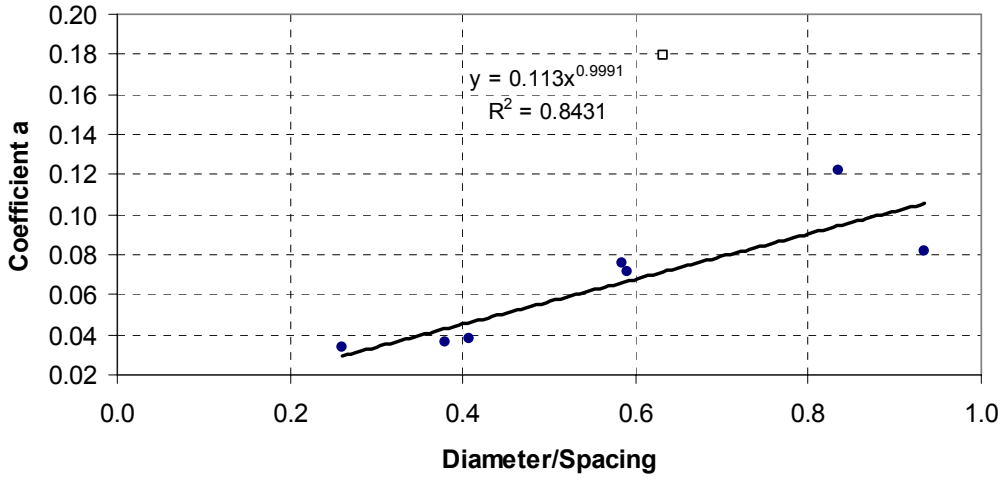


Figure 5.10: Coefficient a vs. ratio of diameter to spacing of hemispheres

Table 5.3: Table listing the fitted data and ignored data when plotting Figure. 5.10

Fitted Data Points		Ignored Data Points	
Coefficient a	$\frac{Diameter}{Spacing}$	Coefficient a	$\frac{Diameter}{Spacing}$
0.072	0.589	0.179	0.633
0.037	0.379	-	-
0.076	0.585	-	-
0.082	0.935	-	-
0.038	0.407	-	-
0.122	0.836	-	-
0.034	0.259	-	-

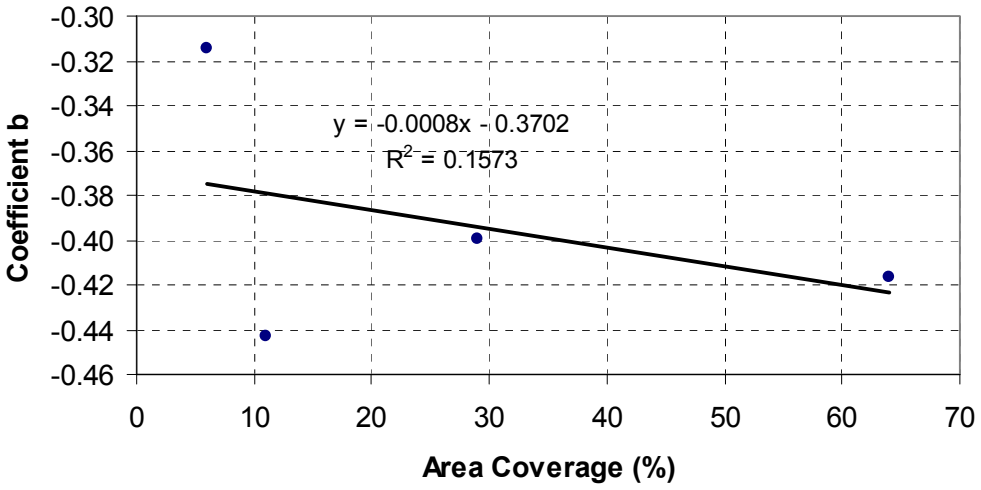


Figure 5.11: Coefficient b vs. Area coverage

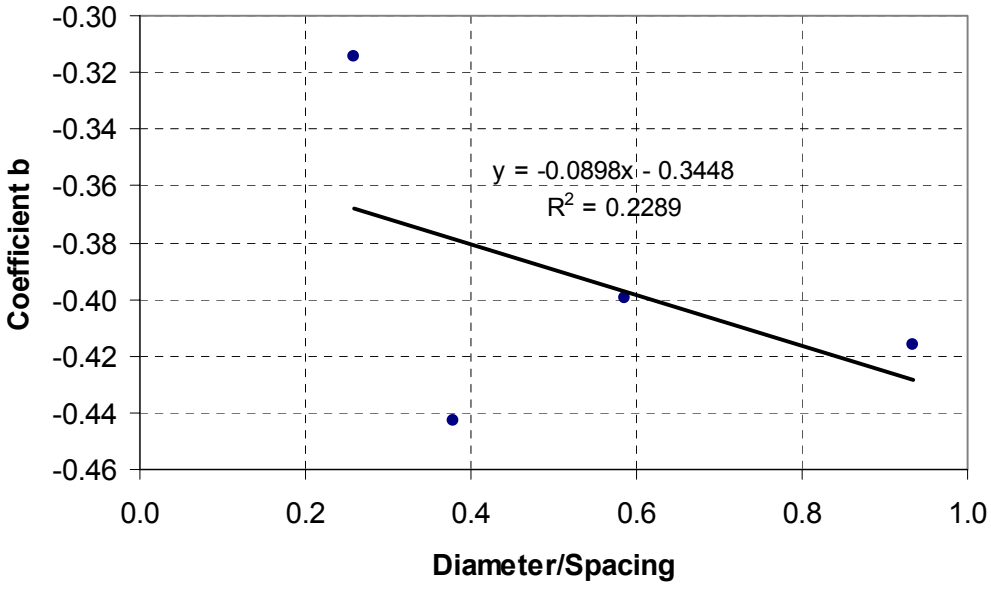


Figure 5.12: Coefficient b vs. ratio of diameter to spacing of hemispheres

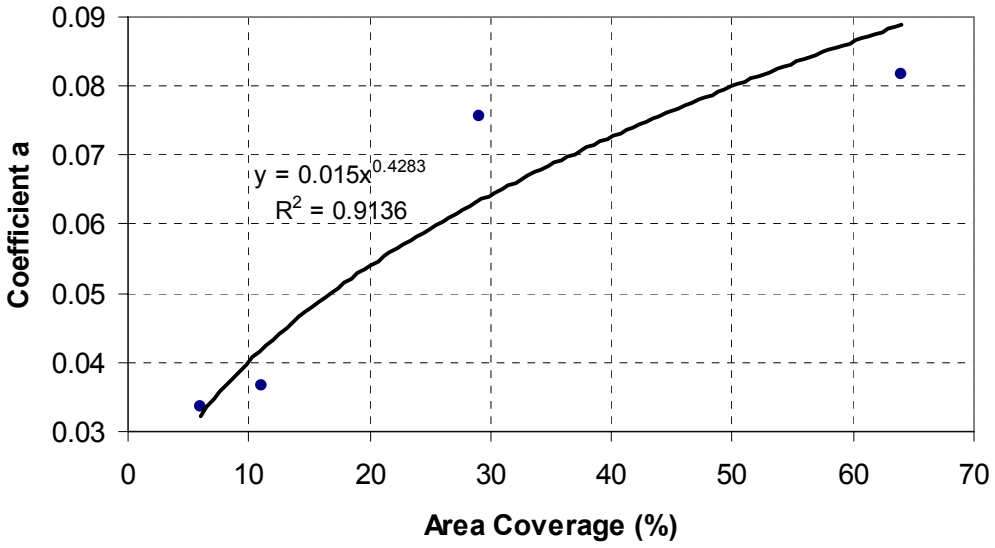


Figure 5.13: Coefficient a vs. Area Coverage

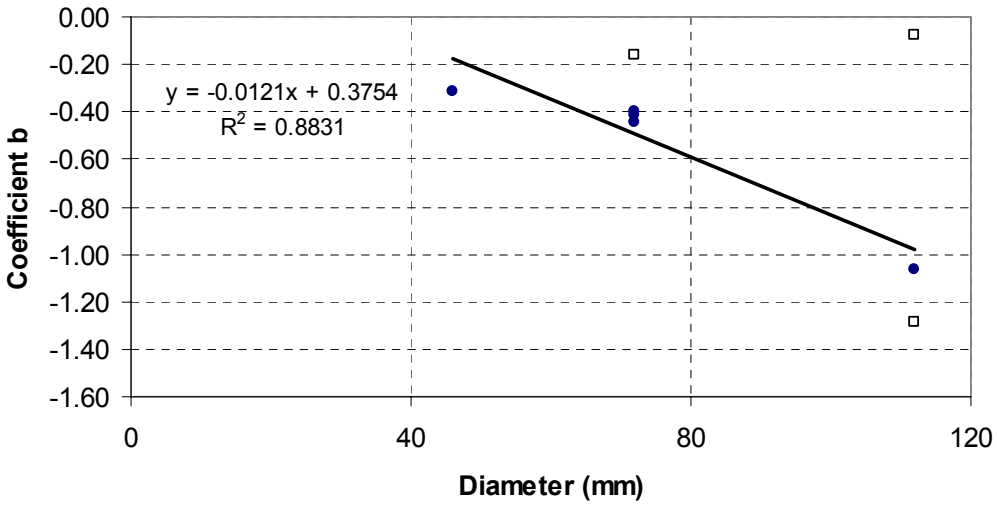


Figure 5.14: Coefficient b vs. Diameter

Table 5.4: Table listing the fitted data and ignored data when plotting Figure 5.14

Fitted Data Points		Ignored Data Points	
Coefficient b	Diameter (mm)	Coefficient b	Diameter (mm)
-1.064	112	-0.162	72
-0.443	72	-0.073	112
-0.399	72	-1.288	112
-0.416	72	-	-
-0.314	46	-	-

When plotting both Figs. 5.10 and 5.14 it was found that the curves do not fit well when the points marked in square shape are included. Therefore those points were removed in order to get the best fitted curves. Figures 5.10 and 5.14 suggest that coefficient a is dependent on the ratio of diameter to spacing, $\frac{D}{Sp}$, and b on the diameter, D of roughness element respectively.

The proposed equation (5.13) was verified by comparison of calculated and predicted values of velocity listed in Appendix B (Table B.1). The experimental data listed in Table B.1 were performed by Jordanova (in preparation) in 12.0 m long and 2.0 m wide flume with a slope of 0.001. These experimental data were used with the permission of Jordanova. Two sizes of hemispheres with diameters of 116 mm and 54 mm were used in modeling river rocks. These hemispheres were arranged in staggered (Tests 1 and 8) and parallel (Tests 6 and 7).

The calculated and predicted velocities as well as r^2 values are presented in Fig. 5.15 and 5.17. Figure 5.15 shows a comparison between the calculated velocities and predicted velocities from series B, C and D. Figure 5.17 indicates a comparison between the calculated velocities and predicted velocities from the experimental data performed by Jordanova (in preparation).

The calculated and predicted resistance coefficients as well as r^2 are presented in Fig. 5.16. Figure 5.16 shows a comparison between the calculated Manning's n and predicted Manning's n. The data used to plot the graphs shown in Fig. 5.15 and 5.16 are given in Appendix B (Table B.2). The minimum errors, maximum errors and average absolute errors for these predictions are given in Tables 5.6 and 5.7.

It can be noted from Figs. 5.15 and 5.17 that the proposed equation (5.13) is the best fitted relationship to the range of conditions tested. The proposed equation (5.13) can therefore sufficiently predict velocity of flow for condition listed in Table B.2 with average absolute error of 17.43 %, and for the condition listed in Table 5.3 with average absolute error of 4.99 %.

Table 5.5: Experimental Data used for Verification of Equation (5.13)

Test	Q (m^3/s)	Flow Depth (m)	Density No./m	Slope	Area Coverage (%)
1 (116 mm)	0.0119	0.064	28	0.001	15
	0.0174	0.074	28	0.001	15
6 (116 mm)	0.0138	0.065	28	0.001	15
	0.0220	0.080	28	0.001	15
	0.0273	0.085	28	0.001	15
7 (54 mm)	0.0070	0.029	28	0.001	3
	0.0100	0.035	28	0.001	3
	0.0129	0.039	28	0.001	3
	0.0171	0.043	28	0.001	3
	0.0217	0.050	28	0.001	3
	0.0276	0.055	28	0.001	3
8 (54 mm)	0.0053	0.025	26	0.001	3
	0.0088	0.032	26	0.001	3
	0.0145	0.040	26	0.001	3
	0.0238	0.052	26	0.001	3
	0.0283	0.056	26	0.001	3

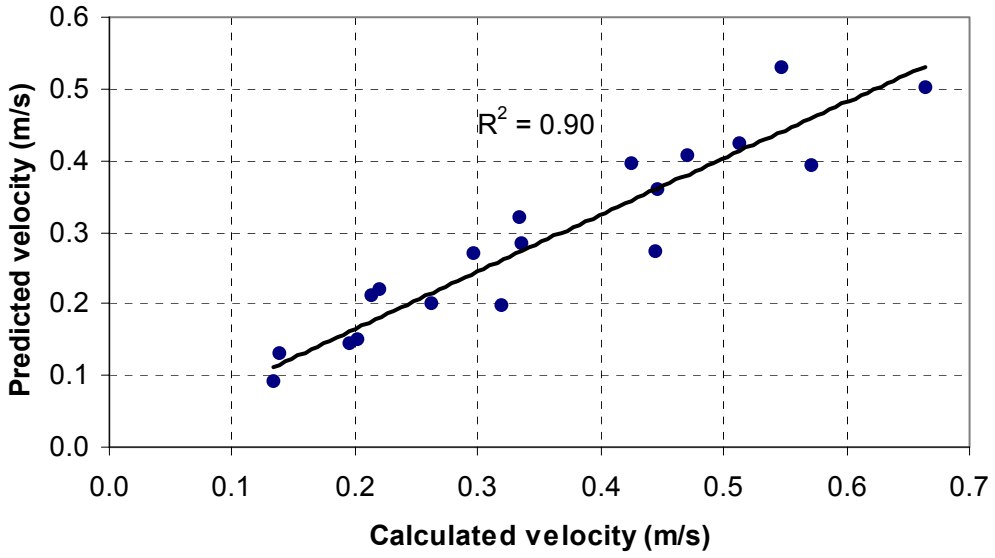


Figure 5.15: Comparison between calculated and predicted velocities for series B, C and D.

The calculated velocity values were computed from equation (5.14) and the calculated Manning's values were computed from equation (5.15).

$$V = \frac{Q}{A} \tag{5.14}$$

$$n = \frac{A^{5/3} S^{1/2}}{Q P^{2/3}} \tag{5.15}$$

where P is the wetted perimeter.

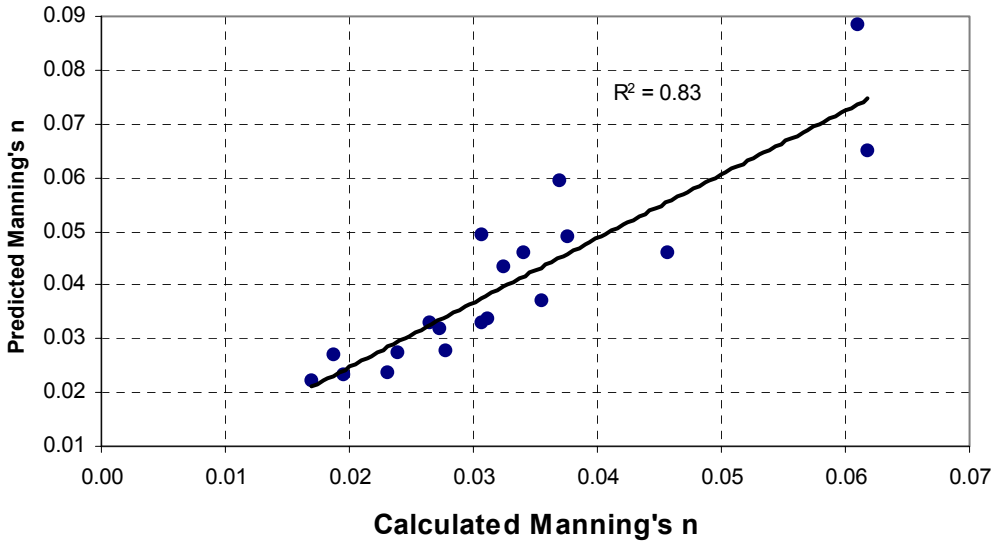


Figure 5.16: Comparison between calculated and predicted resistance coefficient for series B, C and D.

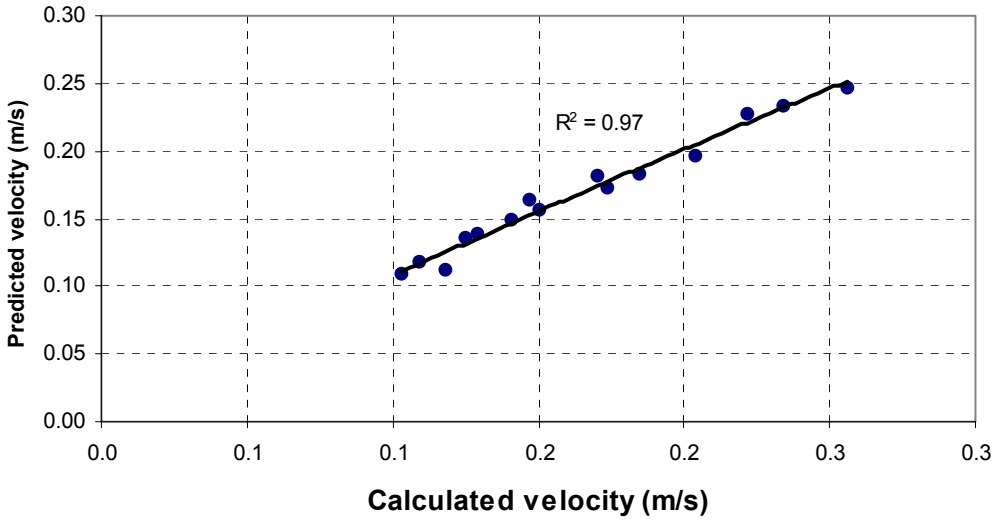


Figure 5.17: Comparison between calculated and predicted velocities for the conditions listed in Table 5.3.

Table 5.6: Velocity Prediction Errors in Application of Equation (5.13) for Series B, C and D (Table A.1 to A.3)

Error	B4	C5	C6	C7	C8	D9
Minimum Error	4.87	14.98	3.02	1.15	31.21	0.38
Maximum Error	23.58	30.92	26.12	6.65	38.33	24.22
Average Absolute Error	15.98	23.68	12.69	3.98	35.88	13.92

Table 5.7: Velocity Prediction Errors in Application of Equation (5.13) for Condition listed in Table 5.3

Error	Test 1 (116 mm)	Test 6 (116 mm)	Test 7 (54 mm)	Test 8 (54 mm)
Minimum Error	-7.41	-4.79	-11.25	-8.30
Maximum Error	-5.49	5.41	-3.84	2.88
Average Absolute Error	6.45	3.53	6.19	3.84

The errors listed in Tables 5.6 and 5.7 gives equation (5.13) allowance for application in intermediate-scale flow condition. The experimental errors shown in Table 5.7 were obtained from the experimental data of Jordanova with conditions different from those listed in Table 5.6.

CHAPTER 6: CONCLUSION

6. Conclusion

Manning's roughness coefficient, n, for a cobble-bed river is not constant, but varies with flow condition. For the range on intermediate-scale conditions tested, Manning's n depends on roughness element size and spacing. Manning's n also depends on the pattern of roughness elements in the transition zone, but not in small scale zone.

The relative size effect depends very significantly on the absolute size (i.e. Manning's n varies with relative submergence much more for large roughness elements than for small ones).

The Manning's n for small scale conditions is dependent on size and pattern of roughness elements. Figure 5.1 shows that the Strickler's equation can be used to predict the n values and that the density of the roughness elements has significant influence on flow resistance (Table 5.1).

The calculated velocities compared well with those predicted by the proposed equation (5.13). The coefficient a is dependent on the ratio of diameter to spacing of roughness elements, whereas coefficient b is dependent on the diameter of roughness elements. The prediction errors give the proposed equation allowance for application in flow conditions with cobble-bed river.

7. References

Ackers, P and White, WR (1973) Sediment Transport: New approach and analysis, Journal of the Hydraulic Division, ASCE, Vol. 99, No. HY11, pp 2041 – 2060.

ASCE Task Force on Friction Factors in Open Channels (1963) Friction Factors in Open Channels, Journal of the Hydraulic Division, ASCE, Vol. 89, No. HY 2, McGraw-Hill.

Bathurst, JC (1978) Flow Resistance of Large-Scale Roughness, Journal of the Hydraulic Division, ASCE, Vol. 104, No. HY 12, pp 1587 – 1603.

Bathurst, JC (1982) Theoretical Aspects of Flow Resistance in Gravel-Bed River, Hey RD.

Bathurst, JC (2002) At - a - Site Variation and Minimum Flow Resistance for Mountain Rivers, Journal of Hydrology, No. 269, pp 11 – 26.

Bayazit, M (1976) Free Surface Flow in a Channel of Large Relative Roughness, Journal of Hydraulic Research, No. 14, pp 115 – 126.

Chadwick, A and Morfett, J (1993) Hydraulics in Civil and Environmental Engineering, Second Edition, New York, Tokyo, pp 116 – 183.

Engelund, F and Hansen, E (1967) A monograph on Sediment Transport in Alluvial Streams, Teknik Vorlag, Copenhagen, Denmark.

French, RH (1985) Open Channel Hydraulics, McGraw-Hill.

Henderson, FM (1966) Open Channel Flow, Macmillan Publishing Co., Inc, New York, pp 125 – 324.

Hey, RD (1979) Flow Resistance in Gravel-Bed Rivers, Journal of the Hydraulic Division, ASCE, Vol. 105, No. HY 4, pp 365 – 379.

James, CS, Birkhead, AL, Jordanova, AA, Kotschy, KA, Nicolson, CR and Makoa, MJ (2001) Interaction of Reeds, Hydraulics and River Morphology, Report No. 856/1/01, Water Research Commission, South Africa.

James, CS and Myers, WRC (2002) Conveyance of one – and two –stage Meandering Channels, Proc. Instn Civ. Engrs Water and Maritime Engineering, Vol. 154, No. 4, pp 265 – 274.

Joranova AA, Birkhead, AL, James, CS and Kleynhans, CJ (2004) Hydraulics for Determination of the Ecological Reserve for Rivers, WRC Report No. 1174, Pretoria, South Africa.

Jordanova, AA (in preparation) Large-Scale Roughness Prediction, Low Flow Hydraulics in Rivers for Environmental Application, WRC Project No. K5/1405.

Kamphius, JW (1974) Determination of Sand Roughness for Fixed Beds, Journal of Hydraulic Research, Vol. 12, No. 2, pp 193 – 203.

Leopold, LB, Bagnold, RA, Wolman, MG and Brush, LM (1960) Flow Resistance in Sinuous of Irregular Channels, Physiographic and Hydraulic Studies of Rivers, U.S. Geological Survey Professional Paper 282-D.

Mahmood, K (1971) Flow in Sand Bed Channels, Water Management Technical Report No. 11, Colorado State University, Fort Collins, Colorado.

Roberson, JA and Wight, SJ (1973) Analysis of Flow in Channels with Gravel-Bed, ASCE, Vol. 27 (11), pp 63 – 72.

Rouse, H (1965) Critical Analysis of Open Channel Resistance, Journal of Hydraulic Division, ASCE, Vol. 91, No. HY 4, pp 1 -25.

Tullis, JP (1966) Free surface effects of the drag of a hemisphere on a boundary in velocity gradient flow, PhD thesis, Utah State University, US.

Thorne, CR and Zevenbergen, LW (1985) Estimating Mean Velocity in Mountain Rivers, Journal of Hydraulic Engineering, Vol. 111, No. 4, pp 612 – 624.

Vanoni, VA and Brooks, NH (1957) Laboratory Study of the Roughness and Suspended Load of Alluvial Streams, Sedimentation Laboratory Report No. E 64, California Institute of Technology, Pasadena, California, U.S.A.

Van Rijn, L (1982) Equivalent Roughness of Alluvial Bed, Journal of Hydraulic Engineering, Vol. 108, No. 10, pp 1215 – 1218.

Yen, BC (2002) Open Channel Flow Resistance, Journal of Hydraulic Engineering, Vol. 128, No. 1, pp 20 – 39.

Appendix A Experimental Data for the Range of Conditions Tested

Table A.1: Experimental Data for Series B Experiments

Density 1				**Spacing = 134 mm**			
Test	Q (m^3/s)	y (m)	y/h	A (m^2)	V (m/s)	S	n
B2.1	0.0044	0.0865	1.5446	0.0239	0.1417	0.0047	0.0736
B2.2	0.0056	0.0905	1.6161	0.0344	0.1624	0.0047	0.0607
B2.3	0.0134	0.1330	2.3750	0.0505	0.2644	0.0047	0.0451
B2.4	0.0192	0.1520	2.7143	0.0578	0.3418	0.0047	0.0386
B2.5	0.0365	0.2095	3.7411	0.0796	0.4718	0.0047	0.0312
B2.6	0.0483	0.2455	4.3839	0.0933	0.5139	0.0047	0.0301
B2.7	0.0546	0.2585	4.6161	0.0982	0.5560	0.0047	0.0282
Density 2				**Spacing = 177 mm**			
B3.1	0.0011	0.0540	0.9643	0.0205	0.0515	0.0047	0.1606
B3.2	0.0065	0.1025	1.8304	0.0390	0.1662	0.0047	0.0637
B3.3	0.0220	0.1520	2.7143	0.0578	0.3963	0.0047	0.0333
B3.4	0.0409	0.2155	3.8482	0.0819	0.5040	0.0047	0.0295
B3.5	0.0474	0.2340	4.1786	0.0889	0.5497	0.0047	0.0277
B3.6	0.0552	0.2555	4.5625	0.0971	0.5685	0.0047	0.0275
Density 3				**Spacing = 190 mm**			
B4.1	0.0030	0.0575	1.0268	0.0219	0.1384	0.0047	0.0618
B4.2	0.0069	0.0765	1.3661	0.0291	0.2624	0.0047	0.0375
B4.3	0.0195	0.1150	2.0536	0.0437	0.4455	0.0047	0.0265
B4.4	0.0315	0.1640	2.9286	0.0623	0.5048	0.0047	0.0269
B4.5	0.0434	0.2005	3.5804	0.0762	0.5701	0.0047	0.0255

Table A.2: Experimental Data for Series C Experiments

Density 1					**Spacing = 190 mm**		
Test	Q (m^3/s)	y (m)	y/h	A (m^2)	V (m/s)	S	n
C5.1	0.0027	0.0350	0.9722	0.0133	0.2014	0.0047	0.0325
C5.2	0.0083	0.0650	1.8056	0.0247	0.3346	0.0047	0.0272
C5.3	0.0197	0.0910	2.5278	0.0346	0.5709	0.0047	0.0187
C5.4	0.0304	0.1255	3.4861	0.0477	0.6372	0.0047	0.0192
C5.5	0.0430	0.1635	4.5417	0.0621	0.6920	0.0047	0.0196
Density 2					**Spacing = 177 mm**		
C6.1	0.0027	0.0360	1.0000	0.0137	0.1958	0.0047	0.0340
C6.2	0.0075	0.0665	1.8472	0.0253	0.2958	0.0047	0.0311
C6.3	0.0181	0.1015	2.8194	0.0386	0.4703	0.0047	0.0238
C6.4	0.0271	0.1360	3.7778	0.0517	0.5477	0.0047	0.0231
C6.5	0.0430	0.1630	4.5278	0.0619	0.6942	0.0047	0.0195
Density 3					**Spacing = 123 mm**		
C7.1	0.0060	0.0745	2.0694	0.0283	0.2132	0.0047	0.0456
C7.2	0.0147	0.1160	3.2222	0.0441	0.3338	0.0047	0.0355
C7.3	0.0238	0.1475	04.0972	0.0561	0.4245	0.0047	0.0307
C7.4	0.0322	0.1740	4.8333	0.0661	0.4868	0.0047	0.0284
C7.5	0.0421	0.2030	5.6389	0.0771	0.5462	0.0074	0.0267
Density 4					**Spacing = 77 mm**		
C8.1	0.0026	0.0515	1.4306	0.0196	0.1327	0.0047	0.0609
C8.2	0.0064	0.0758	2.1056	0.0288	0.2239	0.0047	0.0438
C8.3	0.0138	0.1140	3.1667	0.0433	0.3189	0.0047	0.0369
C8.4	0.0280	0.1655	4.5972	0.0629	0.4447	0.0047	0.0306
C8.5	0.0448	0.2155	5.9861	0.0819	0.5466	0.0047	0.0272
C8.6	0.0498	0.2320	6.4444	0.0882	0.5651	0.0047	0.0269

Table A.3: Experimental Data for Series D experiments

Density 1						**Spacing = 177 mm**	
Test	Q (m^3/s)	y (m)	y/h	A (m^2)	V (m/s)	S	n
D9.1	0.0026	0.0310	1.3478	0.0118	0.2204	0.0047	0.0277
D9.2	0.0115	0.0755	3.2826	0.0287	0.4011	0.0047	0.0244
D9.3	0.0154	0.0790	3.4348	0.0300	0.5134	0.0047	0.0195
D9.4	0.0260	0.1030	4.4783	0.0391	0.6641	0.0047	0.0170

Appendix B Experimental Results for the Predicted Velocities

Table B.1: Experimental Results for the Predicted Velocities

Flume Slope 0.001

Large Hemispheres D (m) 0.116

Small Hemispheres D (m) 0.054

Pattern	Q (m^3)	Y (m)	Y/h	AC (%)	n	V_p (m/s)	V_m (m/s)	Error	ABS Error
	0.0119	0.064	1.032	14.938	0.0446	0.109	0.103	-5.49	5.49
1 (116 mm)	0.0174	0.074	1.194	14.938	0.0384	0.139	0.129	-7.41	7.41
	0.0138	0.065	1.048	14.938	0.0439	0.112	0.118	5.41	5.41
	0.0220	0.080	1.290	14.938	0.0354	0.157	0.150	-4.79	4.80
6 (116 mm)	0.0273	0.085	1.371	14.938	0.0333	0.173	0.174	0.38	0.38
	0.0070	0.029	1.014	3.237	0.0214	0.136	0.125	-9.08	9.08
	0.0100	0.035	1.224	3.237	0.0203	0.164	0.147	-11.25	11.25
	0.0129	0.039	1.364	3.237	0.0197	0.182	0.170	-6.78	6.77
	0.0171	0.043	1.503	3.237	0.0191	0.196	0.204	3.84	3.84
	0.0217	0.050	1.748	3.237	0.0184	0.227	0.222	-2.37	2.37
7 (54 mm)	0.0276	0.055	1.923	3.237	0.0179	0.246	0.256	3.84	3.84
	0.0053	0.025	0.874	3.006	0.0223	0.118	0.109	-8.30	8.30
	0.0088	0.032	1.119	3.006	0.0208	0.150	0.141	-6.37	6.37
	0.0145	0.040	1.399	3.006	0.0195	0.183	0.185	1.19	1.19
	0.0238	0.052	1.818	3.006	0.0182	0.233	0.234	0.45	0.45
8 (54 mm)	0.0283	0.056	1.958	3.006	0.0178	0.251	0.258	2.88	2.88

Table B.2: Experimental Results for the Predicted Velocities

Flume Slope		0.0047
Large Hemispheres	**D (m)**	0.112
Medium Hemispheres	**D (m)**	0.072
Small Hemispheres	**D (m)**	0.046

Test	Q (m^3)	Y (m)	y/h	V_m (m/s)	V_p (m/s)	n_m	n_p	Error	ABS Error
B4.1	0.0030	0.0575	1.0268	0.1384	0.1316	0.0618	0.0649	4.87	4.87
B4.2	0.0076	0.0765	1.3661	0.2624	0.2005	0.0375	0.0491	23.58	23.58
B4.3	0.0195	0.1150	2.0536	0.4455	0.3587	0.0265	0.0329	19.49	19.49
C5.1	0.0027	0.0350	0.9722	0.2014	0.1508	0.0325	0.0435	25.15	25.15
C5.2	0.0083	0.0650	1.8056	0.3346	0.2845	0.0272	0.0320	14.98	14.98
C5.3	0.0197	0.0910	2.5278	0.5709	0.3943	0.0187	0.0271	30.92	30.92
C6.1	0.0027	0.0360	1.0000	0.1958	0.1447	0.0340	0.0460	26.12	26.12
C6.2	0.0075	0.0665	1.8472	0.2958	0.2713	0.0311	0.0339	8.27	8.27
C6.3	0.0181	0.1015	2.8194	0.4703	0.4073	0.0238	0.0275	13.39	13.39
C6.4	0.0283	0.1360	3.7778	0.5477	0.5312	0.0231	0.0238	3.02	3.02
C7.1	0.0060	0.0745	2.0694	0.2132	0.2107	0.0456	0.0461	1.15	1.15
C7.2	0.0147	0.1160	3.2222	0.3338	0.3200	0.0355	0.0370	4.15	4.15
C7.3	0.0238	0.1475	4.0972	0.4245	0.3963	0.0307	0.0329	6.65	6.65
C8.1	0.0026	0.0515	1.4306	0.1327	0.0913	0.0609	0.0885	31.21	31.21
C8.3	0.0138	0.1140	3.1667	0.3189	0.1974	0.0369	0.0597	38.10	38.10
C8.4	0.0280	0.1655	4.5972	0.4447	0.2743	0.0306	0.0496	38.33	38.33
D9.1	0.0026	0.0310	1.3478	0.2204	0.2196	0.0277	0.0279	0.38	0.38
D9.3	0.0154	0.0790	3.4348	0.5134	0.4254	0.0195	0.0235	17.15	17.15
D9.4	0.0260	0.1030	4.4783	0.6641	0.5032	0.0170	0.0224	24.22	24.22